사질토에 있어서 말뚝의 선단부 지지력

End Bearing Capacity of a Pile in Cohesionless Soils.

이 명 환 박사

(한국건설기술연구원, 선임연구원)

End Bearing Capacity of a Pile in Cohesionless Soils

by Myung Whan Lee

ABSTRACT

The aim of this paper is to examine the end bearing capacity of a pile in cohesionless soils. The mode of failure of soil due to pile installation is assumed from experimental observation of actual soil deformation. A new solution is proposed complying with the assumed mode of failure by employing the theory of cavity expansion.

The effect of curvature of failure envelope is studied in relation to the proposed solution. The influence of a curved failure envelope becomes larger with increasing degree of curvature and the level of confining stress. This effect in some cases can reduce the end bearing capacity by more than 80 percent compared with that given by a straight failure envelope.

For practical application of the proposed solution, the method of determining the average volume change in the plastic zone is re-evaluated. The proposed solution is confirmed by comparing the theoretical values with experimental results obtained from model pile tests in a calibration chamber. The comparison shows that the proposed solution provides a reasonable prediction of end bearing capacity for both weak and strong grained soils.

1. Introduction

Since the static method has the advantage of assessing the pile bearing capacity[1] prior to the trial driving or pile load test, it has been widely used in the design of pile foundations. There have been two basic ways of estimating the pile bearing capacity in the static method, namely, the theoretical approach and the empirical approach.

Until recently, the theoretical solutions based on the classic theory of plasticity were frequently considered by the engineers in the design process. In these solutions, the soil is assumed to be a perfect plastic material and the pile bearing capacity depends mainly on the differently assumed failure criteria. Consequently the resulting values differ as much as 100 times and the practicing engineers are more attracted by the variously proposed empirical correlations.

As the requirement for the safer and the more economical ways of constructing pile foundations increased, more attention has been paid for the development of empirical correlations. At the same time, more research effort has been focused on the pile-soil interaction so that a more reliable solution could be developed. The development in the area of in-situ testing methods, especially the cone penetration tests, during the past two decades, provides valuable information in understanding the pile bearing capacity phenomena. The researches confirm that the pile bearing capacity is a function of various soil parameters.

Practically it is not possible to take into consideration of all the influencing factors in a solution, however, it is generally agreed that the two most important soil parameters to be accounted for in a pile bearing capacity solution are the

---

1. In this paper only the cohesionless soil is considered. In cohesionless soils, the side resistance contributes only the small fraction to the total pile bearing capacity, only the end bearing capacity is studied. Hence the terms "soil" and "pile bearing capacity" have been used in lieu of "cohesionless soil" and "end bearing capacity of a pile", throughout the whole text.

shearing characteristics of soil and the soil compressibility. The only theoretical solution which takes the soil compressibility into consideration is the solution based on the theory of cavity expansion. Many reported research confirmed that a more reliable prediction of pile bearing capacity was achieved by means of those solutions based on the theory of cavity expansion. However there are relatively few solutions based on this theory which can be used in practical engineering problems.

In this research, the soil deformation under a pile base is defined by model experiements, and a new theoretical solution is proposed. For the application of the proposed solution in the actual soil model, the effect of curvature of failure envelope has been studied. The verification of the developed theoretical solution was done by comparing the predicted values with the results of model pile penetration tests carried out in a calibration chamber using three different soils of distinctive compressibility characteristics but of apparantly identical shearing characteristics.

2. Review of literature

The limitations of soil mechanics theory in predicting the pile bearing capacity have been repeatedly acknowledged, and, therefore, the current state-of-the-art depends largely on empirical correlations. The vast amount of information available adds to the complexity so that some researchers suggested that a unique law governing the soil-structure interactions in the analysis of pile bearing capacity does not exist (Meyerhof, 1974; Trofimenkov, 1974; Schmertmann, 1975; Mitchell and Lunne, 1978; Villet and Mitchell, 1981; de Ruiter, 1981; Robertson and Campanella, 1983).

Although the state-of-the-art reports on cone penetration testing helps in understanding the pile bearing capacity phenomena, considering the rapid advancement on this subject, it is worthwhile reviewing the available information.

The pile bearing capacity depens on many factors, some of which can be listed as follows :

(1) depth of penetration

(2) stress conditions inside the soil mass

(3) shearing resistance of soil

(4) soil compressibility

(5) stress history, soil fabric, crushability, cementation, etc.

(6) shape and roughness of pile

(7) rate of driving

(8) diameter of pile

Also the following factors have to be considered in laboratory penetration tests :

(9) boundary conditions of soil specimen

(10) relative size of calibration chamber

The review concentrates on the most important of the influencing factors.

2.1 Depth of penetration

According to simple theory the end bearing capacity should increase linearly with increase of overburden pressure or the depth of penetration. There have been some reported cases of linear increase (Plantema, 1957; Janbu and Senneset, 1974; Treadwell, 1975), however, many researchers believe that the end bearing capacity attains its maximum value when a certain relative depth has been reached (Kerisel, 1958; Tcheng, 1961; Vesić, 1963; Biarez and Gresillon, 1972; Peuch et al, 1974).

No satisfactory explanation has yet been made, while an intermediate phenomenon has been reported and generally accepted by many reseachers. A linear relationship between the end bearing capacity and depth of penetration followed by a concave-downwards curve has been prevailing these days (Veismanis, 1974; Holden, 1976; Smits, 1982; Joustra and De Gijt, 1982). It can be explained by introducing the concept of pre-crushing and post-crushing pressure for a certain type of soil grain. Although this helps the understanding the phenomena with respect to some

specific points of interest, a comprehensive explanation can only be made by the thorough understanding of pile-soil interaction which is subject to further study.

2.2 Stress conditions inside the soil mass

In conventional solutions of pile bearing capacity, the vertical effective stress at the level of the pile base has been chosen as the reference value in the analysis of the end bearing capacity. This has sometimes been criticized as it may lead to incorrect results, especially in the case of overconsolidated sands. Schmertmann(1972) suggested from the experimental results that an improved relationship could be established if in-situ horizontal stress was used instead of vertical effective stress. Similar relationships were reported by Houlsby and Hitchman (1988).

However, due to the difficulties in measuring the in-situ horizontal effective stress, not much work has been done to correlate this with end bearing capacity. In the case of overconsolidated sands, improved relationships have been reported when the horizontal effective stress is used in the analyses (Veismanis, 1974; Chapman and Donald, 1981; Villet and Mitchell, 1981; Baldi et al, 1981a).

Some researchers believe that neither the vertical effective stress nor the horizontal effective stress is appropriate in assessing pile bearing capacity. The mean normal stress has been used in the solutions based on the theory of cavity expansion (Vesić, 1972; Al Awkati, 1975) which have been widely recognized as giving an improved correlation and consequently have been preferred by many researchers (Baldi et al, 1981a; Robertson and Campanella, 1983; Mitchell and Keaveny, 1986; Tomlinson, 1987).

2.3 Shearing characteristics of soil

Most of the analytical solutions for pile bearing capacity in cohesionless soils are based on the theory of plasticity in which the shearing strength is defined by the Mohr-Coulomb failure criterion.

$$\tau = \sigma \tan \phi \quad [1]$$

In the theory of plasticity the soil is assumed to be a perfect plastic material and the volume change is not allowed. Consequently the angle of sharing resistance, ϕ, is the only variable considered.

The general approach of assessing pile bearing capacity is to assume a certain mode of failure which is more or less related to that of a shallow foundation. Since the classic work of Prandtl(1920) which provided a theoretical basis for many other solutions, there have been many proposals based on differently assumed ship surfaces. Some of the well-known solutions are shown in Fig.1.

As well-explained in a paper by Vesić(1967), the resulting values from these well-known theoretical solutions differ as large as 100 times and can not be used in a practical engineering problem. It can, therefore, be postulated that a solution which takes into account of the angle of shearing resistance, as the only variable considered, can not provide a universal answer for the pile bearing capacity problem.

In Fig.2, the results of some well-known theoretical solutions are shown together with some empirical correlations. As shown in the figure, it does not seem possible to predict pile bearing capacity from these relationships. It is obvious that a unique relationship between angle of shearing resistance and pile bearing capacity does not exist.

---

1. Since the research deals with dry soil, only the effective stress is concerned. Therefore the symbols "ϕ" and "σ" are used in place of "ϕ'" and "σ'" throughout the text.

2.4 Soil compressibility

The effect of soil compressibility on pile bearing capacity has been considered by many researchers. The differences in Fig.3, cannot be explained unless analysed in terms of soil compressibility. Veismanis(1974) reported similar phenomena (Fig.4), but the most appealing comparison was made by Vesić(1964) which is shown in Fig.5. By mixing 10 percent of mica with Chattahoochee sand, soil compressibility changed significantly, while the shearing characteristics remained more or less the same. Bhushan(1970) produced some interesting comparisons of the effect of each soil parameter from the viewpoint of limit cavity expansion pressure.

All the foregoing discussions lead to one definite conclusion. In the analysis of pile bearing capacity, all the factors which affect the pile bearing capacity should be taken into account, because solutions which ignore some of the important factors may be in serious error.

3. Theoretical consideration

From what have been discussed in the previous chapter, the limitations of the theoretical solutions based on the theory of plasticity are quite clear. Therefore the theoretical approach in this research is made from the viewpoint of the theory of cavity expansion where both of the two most important soil parameters are considered. In practice, the pile bearing capacity solutions based on the theory of cavity expansion have gained reputation that much improved correlation was obtained when the results were compared with those obtained from solutions based on the theory of plasticity (Baldi et al, 1981b; Robertson and Campanella, 1983; Mitchell and Keaveny, 1986).

In reality, however, there have been quite few solutions available which are based on the theory of cavity expansion. The only purely theoretical solution in this respect is the one proposed by Vesić(1977) which has been repeatedly criticized

to result in higher values of end bearing capacity (Baldi et al, 1981b; Robertson and Campanella, 1983; Mitchell and Keaveny, 1986). The other semi-empirical solution by Al Awkati(1975) is subject to a serious discrepancy between the assumption and the fact which has been proved later experimentally. Mitchell and Keaveny(1986) tried to improve the solution by introducing the concept of cylindrical cavity expansion, which is hardly regarded as a fundamental solution. It was, therefore, concluded that the cavity expansion solution should be re-evaluated by examining the mode of deformation under the pile base.

3.1 Soil deformation under the pile base

There have been many attempts to define the movement of soils under the pile base, but most of them suffer from the restrictions of chamber size effect and boundary conditions effect. The visual evidences of shear plane as interpreted from discontinuities of soil layer observed in a glass-walled soil container with a half-section of a model pile or in a detachable box with a penetrating wedge (Durgunoglu, 1972) should be re-evaluated.

The radiographic observation by Robinsky and Morrison(1964) also suffers from the restrictions, however, considering the relative density of the soil specimen and the relative dimension of the testing apparatus, the results are probably acceptable(Fig.6). The drawn conclusions are as follows :

(1) The soil deformation due to a pile installation is limited by a barrel shaped envelope.

(2) A cone-shaped zone develops beneath the pile base which is believed to be the main compaction zone.

(3) Below the pile base the envelope is roughly spherical.

(4) The general shape of the envelope remains the same, whilst its size varies with pile diameter, pile taper, pile surface roughness and the relative

density of the sand.

(5) The maximum depth of the envelope below the pile base varies from about 2.5 to 4.5 times the pile diameter for the range of tests performed.

The experimental findings of a spherically deformed zone under the pile base and a cone-shaped main compaction zone provides a valuable insight in relation to cavity expansion theory. Similar shaped core was observed by Koizumi et al(1971) under an actual pile.

Al Awkati's(1975) explanation generally coincides with above (Fig.7). As the pile penetrates, a bullet-shaped "failure front" is formed and advances with the penetrating pile. The soil element formerly outside the "failure front" changes from a state of elastic to plastic equilibrium and the level of stress is increased. As the pile penetration continues, the stress level above the pile reduced significantly.

3.2 Assumed mode of deformation

To investigate the mode of deformation, model tests were performed using a resin impregnation technique. The details are given later in this paper. The results of model tests which were more or less similar to the results of Robinsky and Morrison(1964) could not provide the necessary quantitative information required, but were sufficient enough to assume a new mode of deformation (Fig.8).

It is assumed that the process of an advancing pile creates a state inside the soil mass which is similar to the process of an expanding spherical cavity. This assumption does not seem to deviate from the actual case, since the reported dimension of deformed zone by Robinsky and Morrison(1964) coincides reasonably with the reported typical dimension of a spherical plastic zone by Vesić(1972).

As the pile pentrates, a core in the shape of a half-sphere begins to form. As the penetration continues, the zone around the core begins to change from an initial elastic state to a plastic one. The boundary of the plastic zone which is also in

the shape of a half-sphere, continues to expand as the pile continues to penetrate until an ultimate dimension is reached. At that time the cavity expansion pressure reaches its maximum value.

Fig.9 shows the stress distribution in the plastic zone. Since the core is assumed to be the expanding cavity, the stress at the boundary of the cavity would be the limit spherical cavity expansion pressure, p_u. To make the problem simple, a correlation factor, ζ, is introduced, then the end bearing capacity, q_b, can be expressed by following equations :

$$q_b = N_\sigma \cdot q \qquad (1)$$

$$q_b = \zeta \cdot p_u \qquad (2)$$

$$p_u = F_q \cdot q \qquad (3)$$

$$N_\sigma = \zeta \cdot F_q \qquad (4)$$

where q_b = end bearing capacity

N_σ = bearing capacity factor in terms of mean normal stress

q = initial mean normal stress

ζ = correlation factor between spherical cavity expansion pressure and end bearing capacity

p_u = limit spherical cavity expansion pressure

F_q = spherical cavity expansion factor

Therefore the problem of end bearing capacity reduces to the calculation of the spherical cavity expansion factor, F_q, and the correlation factor, ζ.

3.3 Expansion of a spherical cavity

A spherical cavity of an initial redius, R_i, is assumed to expand due to an internal pressure, p. As the pressure increases, the cavity is expanded and the soil around the cavity will be changed from the initial isotropic state to a state of plastic equilibrium. The expanding process will be continued until the internal

pressure reaches its maximum value. When the pressure reaches its maximum value, the plastic zone will have a limiting radius, R_u, and beyond this zone the soil remains in its initial state of elastic equilibrium (Fig.10). In the solution by Vesić (1972), the followings were assumed:

(1) The soil inside the plastic zone behaves as a compressible plastic solid and its characteristics are defined by an angle of shearing resistance, ϕ, and by an average volumetric strain, Δ.

(2) In the zone of elastic equilibrium, its characteristics are defined by a Young's modulus, E, and a Poisson's ratio, ν.

(3) Before the expansion takes place, the soil is assumed to be under an isotropic effective stress, q, and the body weight of the soil is assumed to be negligible when compared with the applied pressure. Therefore a weightless spherically symmetric model is considered, and the shearing stress on the soil element (Fig.10) is eliminated.

The solution by Vesić(1972) is perfectly valid and is summarized in Table 1. Figs.11 and 12 are the calculated spherical cavity expansion factor, F_q, for the strong and the weak grained soil.

3.4 End bearing capacity of a pile

At the boundary between the core and the plastic zone, the radial stress will have a value, $\sigma_r = p_u$ (Fig.9), and the soil inside the core is subject to an all-round isotropic compression condition. Since the stress condition inside the core is very difficult to define, until a suitable method is developed, a simplifying assumption would be necessary. It is thus assumed that the behavior of the soil inside the core can be simulated by a process of a triaxial compression condition in which the soil is initially compressed by an isotropic compression pressure and later subject to shear. In this way, the end bearing capacity can be calculated from the Mohr's

circle in which the minor principal stress is the limit spherical cavity expansion pressure and the major principal stress would be the end bearing capacity. The relationships are expressed as follows :

$$q_b = \zeta \cdot p_u \qquad (5)$$

$$\zeta = \frac{1 + \sin\phi}{1 - \sin\phi} \qquad (6)$$

$$p_u = q \cdot F_q \qquad (7)$$

Proposed relationships of correlation factor are shown in Fig.13 and the calculated bearing capacity factor, N_σ , are shown in Fig.14. For comparison purposes, various suggested correlation factors by other researchers are also shown in the figure. One point to be mentioned at this stage is that the above results are based on the assumption of the straight failure envelope. Actual estimation of end bearing capacity should be done by a procedure which takes account of the real soil behaviour.

3.5 Curvature of failure envelope

In most cohesionless soils the failure envelope of the Mohr's circle is not straight but curved. This phenomenon has been well recognized since the early time of soil mechanics, but most of the theoretical solutions neglect this point. The stress level below the pile base usually reaches a value which is much higher than the level frequently encountered in common geotechnical engineering practice. Therefore the effect of a curved failure envelope could be a vital one, however, there does not seem to be much work on this subject except by Baligh(1976).

3.5.1 Curved failure envelope

In Fig.15, a typical curved failure envelope is shown. Since it is usual to have a linear relationship if $\tan\phi$ is plotted against $\log\sigma$, the curvature can be

expressed. Baligh(1976) suggested a practical way to define the relationship by introducing an arbitrary reference stress, q_o , to get a dimensionless relationship which is expressed as :

$$\tan\phi_s = \tan\phi_o + \tan\alpha\left(\frac{1}{2.3} - \log\frac{q}{q_o}\right) \qquad (8)$$

where ϕ_s = secant angle of shearing resistance

ϕ_o = representative angle of shearing resistance defined at $\sigma = 2.72\, q_o$

α = degree of curvature of failure envelope

q = level of stress to be considered

q_o = arbitrary reference stress chosen as 100 kPa

The studies of granular material at elevated stress (Billam, 1971) showed that beyond a certain stress level, the value of ϕ does not decrease but approaches to a constant value which coincides with the angle of intergranular friction, ϕ_μ. This point should be considered in the solution (Billam, 1977), therefore the above equation (8) should be limited by the following equation.

$$\phi_s < \phi_\mu \qquad (9)$$

3.5.2 Calculation procedure

Since the Mohr-Coulomb failure criteria should be satisfied at every point in the plastic zone, it would be impossible to analyse the effect of curved failure envelope precisely. An approximate procedure has been developed making use of the fact that the circumferential stress does not vary much with change of angle of shearing resistance while the radial stress changes sharply. The calculation procedure is summarized in Table 2. The calculation was done by a computer program, DISTRIB, and the results are presented by introducing a correction factor, β, defined as,

$$\beta = \frac{P_u \text{ for curved failure envelope}}{P_u \text{ for straight failure envelope}} \qquad (10)$$

Hence the bearing capacity factor, N_σ^*[1], and the spherical cavity expansion factor, F_q^*, are expressed as follows :

$$F_q^* = \beta . F_q \qquad (11)$$

$$N_\sigma^* = \zeta^* . F_q^* \qquad (12)$$

$$N_\sigma^* = \zeta^* . \beta . F_q \qquad (13)$$

3.5.3 Correction factor, β

The correction factor depends on the following parameters :

(1) secant angle of shearing resistance at the stress level of 2.72 q_o, Φ_s

(2) degree of curvature of failure envelope, α

(3) reduced rigidity index, I_{rr}

(4) mean normal stress prior to pile installation, q

(5) intergranular friction angle, Φ_μ

The results obtained are more or less the same as those proposed by Baligh(1976), however, the main differences are from the condition imposed by equation (9). This is shown clearly in Figs.16 and 17.

3.5.4 Correlation factor, ζ^*

Correlation factor depends mainly on the limit spherical cavity expansion pressure, which depends on many soil parameters. Therefore, the variation is quite complicated to define, and only a possible range of variation is shown in Fig.18. Theoretically, it is possible to have a higher value of correlation factor than appears in the figure, at a very shallow depth of penetration. However, for most of the practical deep foundation problems, the uppermost curve in the figure, which is the corresponding curve for $\alpha = 0^\circ$ case, would serve as the upper limit. The lowermost line, corresponding the intergranular friction angle, would be the lower limit. For

---

1. The symbol used for the case of the curved failure envelope are used with a mark "*" to distinguish them from those symbols used for the case of the straight failure envelope.

a certain value of ϕ_o, the correlation factor becomes less as (1) the I_{rr} value increases, (2) the α value becomes larger and (3) the level of initial stress becomes greater.

The results are compared with the suggested relationships of other researchers (Fig.19). The proposed relationship gives much lower value than Vesić's which has repeatedly reported to overestimate the end bearing capacity. Mitchell and Keaveny(1986) solved the problem by making use of the Meyerhof's(1951) general bearing capacity factor for a shallow foundation as a correlation factor. This helps to reduce the end bearing capacity, but only in the case where ϕ_s value is very low. At higher ϕ_s values, their suggested correlation factor exceeds the one suggested by Vesic(1977). Since the criticism of Vesić's solution has mainly been reported in the cases of higher ϕ_s values, their treatment did not improve but made the problem more serious. They solved this by suggesting the use of cylindrical cavity expansion factor instead of spherical one, if the I_{rr} value exceeds 250. However, this causes uncertainties regarding the actual application. For example, the corresponding bearing capacity factor for I_{rr} = 300 and I_{rr} = 500 are less than those of I_{rr} = 100 and I_{rr} = 200, which obviously is not acceptable.

Even though the relationships by Al Awkati(1975) seem to remain within the reasonable range of the proposed solution, the relationships are not acceptable since the correlation factor increases with increasing I_{rr} values. The experimental findings as well as the theoretical consideration clearly indicates that the correlation factor decreases with increasing I_{rr} values for most of the actual soil model where failure envelope is curved.

3.5.5 Bearing capacity factor, N_σ^*

Typical results are shown in Figs.20 and 21. As shown in the figures, the effect of curved failure envelope reduces the end bearing capacity by as much as 80

percent. It is, therefore, concluded that the effect of curvature of failure envelope should not be neglected and each case should be analysed taking all the relevant parameters into consideration.

4. Experimental work

To study the mode of failure, model tests were performed using resin impregnation technique. The validity of the proposed solution was confirmed by comparing the results obtained from the model pile penetration tests. To analyse the results, soil parameters were determined from standard laboratory tests.

4.1 Materials tested

In the choice of the material, soil compressibility was the prime concern so that its effect could be visualized. Three different soils were used : Leighton Buzzard sand(quartz sand), crushed anthracite and crushed chalk. These three materials were chosen especially because of the similarities in their shearing characteristics whilst their compressibility characteristics show large variations. According to Billam(1971), the particle strengths are in the ratio of 200:13:1.

4.2 Standard tests

To have the mechanical soil parameters,following standard tests were performed :

(1) specific gravity tests

(2) particle size distribution tests

(3) maximum and minimum porosity tests

(4) isotropic compression tests

(5) one-dimensional compression tests

(6) triaxial compression tests

(7) $K_o$compression tests

4.3 Mode of deformation tests

There have been several possible ways to investigate the deformation inside the soil mass during penetration of a pile. Summaries of these methods are as follows :

(1) Direct optical measurement of soil deformation using a glass-walled rigid box with a half-section model pile (Berezantzev et al, 1957; Butterfield and Andrawes, 1972; Koumoto and Kaku, 1982; Davidson et al, 1981)

(2) Observation of undisturbed cross section (Vesić, 1963; Durgunoglu, 1972)

(3) Observation of radiographs (Robinsky and Morrison, 1964; Steenfelt et al, 1981)

(4) Photoelastic investigation making use of optically measurable particles (Allersma, 1982)

All of the methods are subject to the limitation of rigid boundary conditions. To overcome this problem, model pile tests were performed inside a rubber membrane which is surrounded by water. An ordinary triaxial cell was modified and both the natural and coloured specimen were deposited with the experimental set up as shown in Fig.22. After the polypropylene model pile being driven the specimen soil was hardened by acetone solution with 5 percent cellulose acetate dissolved. Later the hardened specimen was recovered and impregnated with resin (ARALDITE HY 1300 + ARALDITE CY 1301). The impregnated specimen was cut into halves with a diamond saw and the deformation was examined.

4.4 Model pile penetration tests

Even though there are many uncertainties in the transposition of a penetration resistance obtained with a reduced scale model to a pile bearing capacity, a penetration resistance is generally accepted to represent a pile bearing capacity. To simulate the actual site condition in a laboratory test, a calibration chamber was designed and fabricated (Fig.23). In the design of a calibration chamber, the

boundary conditions effect and the calibration chamber size effect were considered. The details of these effects are found elsewhere (Holden, 1971; Parkin, 1977 and 1982; de Ruiter, 1981; Lee, 1987).

A flat ended model pile was so designed that both the end bearing and the total resistance could be recorded separately. The specimen soil was deposited by a pluviating method and both the vertical and lateral pressure were applied and maintained for 24 hours before the penetration took place. Penetration resistance was recorded by means of an experimental set-up as shown in Fig.24. The details regarding the testing technique is found in Lee(1987), and Table 3 gives the summaries of the tests performed.

5. Test results and discussion

5.1 Determination of Young's modulus, E

Young's modulus was determined from the initial straight line relationship between the deviator stress and the axial strain of a triaxial test. However, the choice of an appropriate Young's modulus value requires further consideration since the stress path taken in a triaxial compression test differs from that of the spherical cavity expansion. According to the theory of cavity expansion, at the boundary between elastic and plastic zones, failure takes place at a constant mean normal stress equivalent to the initial isotropic stress. In the elastic zone, away from the expanding cavity the soil is subject to an initial isotropic stress. In a routine triaxial compression test, however, the soil is first consolidated at a constant cell pressure then sheared to failure. Bhushan(1970) made this point clear and suggested that the Young's modulus as determined from a triaxial compression test should be used with the condition that the mean normal stress at failure is equal to the initial isotropic stress in a cavity expansion process. Hence the Young's modulus values were determined accordingly and Fig.25 shows the summary of the test

results of three materials.

5.2 Determination of Poisson's ratio, ν

According to the study of influence of each parameter on end bearing capacity (Bhushan, 1970; Lee, 1987), the variation of Poisson's ratio does not cause any significant difference of final result. It is a usual procedure to assume a certain generally acceptable value of Poisson's ratio in the calculation, if the information is not available. In this research, Poisson's ratio was calculated from the relationships between Young's modulus as obtained in 5.1 and the bulk modulus obtained from isotropic compression tests.

5.3 Determination of ϕ_0 and α

The results of triaxial compression tests on three different soils indicate that the failure envelopes are not straight, but curved. The values of ϕ_0 and α were determined with the procedure as discussed in 3.5. Fig.26 is the summarized results of the tests.

5.4 Determination of average volumetric change in plastic zone, Δ

Average volume change in the plastic zone contributes to end bearing capacity in determining the reduced rigidity index which is expressed as,

$$I_{rr} = I_r / (1+I_r \Delta)$$

The introduction of volume change in the theory of pile bearing capacity (Vesić, 1977) improves the theory. However the application of this concept is limited by the nature of the above equation, since the equation holds only for positive (compressive) values of volume change. Negative values of volume change may result in negative values of reduced rigidity index, which is not acceptable. In practice, most sands expands during shearing, consequently the average volume change becomes

negative. Vesić(1972) suggested to using only the positive value of volume change for the above equation. In cases of negative volume change, the value should be taken as zero.

Due to the presence of rigid pile body above the underlying plastic zone, it is not possible to determine the average volume change theoretically. Neither is possible to determine it experimentally with the present state-of-the-art. An alternative way to determine this value is making use of the results obtained from a series of triaxial compression test (Bhushan, 1970; Vesić, 1972).

A typical curve used in conventional volume change estimation is shown in Fig.27(a). The resulting volume change value according to this curve would be positive (compressive). This conclusion is questionable since the solution does not take into consideration of the actual volume of soil which is subject to the volumetric strain. The same curve becomes quite different if the volumetric strain is plotted against radial distance (Fig.27.b). Fig.28 shows the areas of compression and dilation for the same curve. If the three-dimensional aspect of the spherical plastic zone is considered, the volume of soil where compression takes place would be much smaller.

As discussed above, the actual estimation of average volume change is almost impossible. Until a suitable method is developed, it is suggested that following tentative conclusions be used in the calculation of end bearing capacity :

(1) The actual volume change is more dependent on the volumetric strain conditions of the outer part of the plastic zone, where the level of stress is relatively low. Therefore the realistic average volume change would be much smaller than the value obtained by the conventional method.

(2) For practical application to strong-grained soils which usually show dilatancy, the method of estimation does not cause any difference in the final result, because negative volume change is not allowed in the

solution. Consequently the average volume change would be zero in any cases.

(3) For weak-grained soils, a practical suggestion is to assume $\Delta = 0$ for the calculation until a more suitable method is developed. This assumption would not cause any significant errors, since the effect of volume change is not great for soils of lower rigidity index which is usual for weak-grained soils.

5.5 Examination of soil deformation around the pile tip

The resin impregnated specimen was cut into halves and the surface was polished to have a clear observation of the deformation. The observed deformation was more or less the same as the result reported by Robinsky and Morrison(1964). The details regarding the test results are found in Lee(1987).

5.6 Measured base resistance

A similar phenomenon was observed in all the tests performed. After a sharp increase of base resistance with increasing depth of penetration, the base resistance reaches its maximum value. Further penetration does not cause much variation of the maximum value. Hence the determination of the representative end bearing capacity value is easy, by taking the average value of the base resistance once it is seen to reach a constant value.

Fig.29 shows the typical penetration curves of quartz and (K_o=0.415), and Fig.30 shows the typical curves of anthracite (K_o=1.0). Summaries of the test results are shown in Fig.31 where the base resistance is plotted against the mean normal stress. The bearing capacity factor was calculated and the results are shown in Fig.32. The relationships for quartz sand and crushed chalk are more or less linear while those of crushed anthracite are non-linear. As the apparant shearing characteristics of

the three tested soils are broadly similar, the differences between these curves cannot be explained by the classic theory of plasticity.

5.7 Effect of K_o value

Conventionally the vertical effective stress has been regarded as the reference stress for calculating the end bearing capacity. Some researchers suggested the use of in-situ horizontal stress in the calculation while the mean normal stress has been chosen in the theory of cavity expansion. It seems that the argument of what stress should be used in end bearing capacity calculation has not yet been finalized.

The test results obtained from two different stress conditions - isotropic and K_o=0.415 stress condition- are studied in this regard. Fig.33 is the base resistance divided by vertical effective stress plotted against the depth of penetration. The results are clearly separated by the imposed stress conditions. As expected the results of isotropic stress condition gives higher value than K_o stress condition. It is evident that end bearing capacity estimation based on vertical effective stress cannot provide a consistent result and an additional empirical correction factor is needed to predict the end bearing capacity at different K_o values.

The use of horizontal effective stress is not satisfactory either as shown in Fig.34. As expected, a higher K_o value results in lower end bearing capacity, and a general relationship cannot be achieved.

In Fig.35 the base resistance is divided by mean normal stress, and the two different stress conditions give very similar result. In detail, however, the two groups of curves are not the same. The curves of $K_o$stress condition show a definite plateau while those of isotropic stress condition show a less pronounced one. The detailed analysis of the difference may require further research. It is, however, concluded that the foregoing discussion is enough to accept the using of mean normal stress in end bearing capacity calculation.

5.8 Comparison of predicted and measured end bearing capacity

End bearing capacity was calculated by the proposed solution using the soil parameters as previously determined. To compare the proposed solution with other solutions based on the cavity expansion theory, the end bearing capacity was calculated by several different solutions. The solutions considered in the comparison as well as the symbols used are summarized in Table 4.

The predicted end bearing capacity by the considered solutions and the measured value are shown in Figures 36 to 43, and in Fig.44 all the predicted values for three different soils are presented. Since all the solutions are based on the theory of cavity expansion, the differences are due to the differences of correlation factors. As shown in figures, the general trend of each solution is the same regardless of the type of soil. From the comparison, the following conclusions are drawn.

(1) Vesić's original solution (1977) overestimates the end bearing capacity. Correction for the effect of curvature of failure envelope improves the prediction, but it still overestimates the end bearing capacity.

(2) The proposed solution by Mitchell and Keaveny(1986), based on experimental findings, improves the prediction and the correction for the effect of curved failure envelope significantly improves the prediction. However, the condition of application suggests that the overestimation would be higher and more serious as the reduced rigidity index becomes higher. Using the cylindrical cavity expansion model in place of the spherical one does not seem to provide a fundamental solution to the overestimation problem, because the transition causes contradictions.

(3) The semi-empirical correlation suggested by Al Awkati(1975) does not agree with the experimental findings of Mitchell and Keaveny(1986). According to the solution, the correlation factor increases with increase of reduced rigidity index, which is contrary to the theoretical consideration made in

this research. Despite the foregoing contradictions, the solution provides quite reasonable predictions within the scope of this research. However, like the case of Mitchell and Keaveny's, the prediction would be much higher for soils of higher reduced rigidity index values.

It is evident from the results of this experiment that a bearing capacity solution should take both the shearing and soil compressibility characteristics into account. A reasonable prediction of end bearing capacity by most of the available theoretical solutions is not possible for the type of soils studied in this research.

6. Conclusions

1. A new mode of deformation in connection with pile penetration is established by assuming a spherical plastic zone around the pile base. The soil deformation in the plastic zone is assumed to be a process of expanding a spherical cavity.
2. Based on this mode of deformation, a new theoretical solution is proposed. In this solution, the end bearing capacity is divided into two components - a spherical cavity expansion pressure and a correlation factor. The spherical cavity expansion pressure is calculated by the theory of cavity expansion. The correlation factor is calculated by assuming a triaxial compression condition in the core.
3. In most practical soils, the failure envelope is curved. The effect of curvature of failure envelope on end bearing capacity depends on many parameters and should be considered in the pile bearing capacity solution.
4. Since various factors contribute in the determination of end bearing capacity for the cases of actual soil model where the failure envelope is curved, it is not possible to express in a simple mathematical form. Actual calculation can be made by interpolating the typical values as presented in Lee(1987).

5. In the calculation, the actual soil behaviour - a constant value of angle of shearing resistance beyond a certain critical stress level - should not be neglected.
6. The conventional method of estimating the average volume change in the plastic zone is re-evaluated. It is not possible to predict the actual volume change, however, until a suitable method is developed it is suggested that the average volume change should be taken as zero, which would not cause any difference.
7. Most of the available solutions based on the classic theory of plasticity ignore the effect of soil compressibility. Consequently the application of these solutions is limited and cannot be relied on especially for compressible soils.
8. The proposed solution provides a reasonable prediction of end bearing capacities of three different soils.

REFERENCES

ABBREVIATIONS

A.S.C.E.	American Society of Civil Engineers
E.S.O.P.T.	European Symposium on Penetration Testing
I.C.S.M.F.E.	International Conference on Soil Mechanics and Foundation Engineering
N.G.I.	Norwegian Geotechnical Institute
Proc.	Proceedings.

Al AWKATI, A., 1975. On problems of soil bearing capacity at depth. Ph.D. Thesis, Duke University, Durham, NC (unpublished).

ALLERSMA, H.G.B., 1982. Photoelastic investigation of the stress distribution during penetration. Proc. 2nd E.S.O.P.T., Amsterdam, Vol.2, 411-418.

BALDI, G., BELLOTTI, R., GHIONNA, V., JAMIOLKOWSKI, M. and PASQUALINI, E., 1981a. Cone resistance of a dry medium sand. Proc. 10th I.C.S.M.F.E., Stockholm, Vol.2, 427-432.

BALDI, G., BELLOTTI, R., GHIONNA, V., JAMIOLKOWSKI, M. and PASQUALINI, E., 1981b. Cone resistance in dry N.C. and O.C. sands. Proc. Cone Penetration Testing and Experience, Geotechnical Engineering Division, A.S.C.E., 145-177.

BALIGH, M.M., 1976. Cavity expansion in sands with curved envelopes. Proc. A.S.C.E., Vol.102, GT11, 1131-1146.

BEREZANTZEV, V.G. and YAROSHENKO, V.A., 1957. The bearing capacity of sand under deep foundations. Proc. 4th I.C.S.M.F.E., London, Vol.1, 283-286.

BHUSHAN, K., 1970. An experiemental investigation into expansion of spherical and cylindrical cavities in sand. Ph.d. Thesis, Duke University, Durham, N.C. (unpublished).

BIAREZ, J. and GRESILLON, J.M., 1972. Essai et suggestions pour le calcul de la force portante des pieux en milieu pulverulent. Géotechnique, Vol.22, No.2, 433-450

BILLAM, J., 1971. Some aspects of the behaviour of granular materials at high pressures. Proc. Roscoe Memorial Symposium, Cambridge University, 69-80.

BILLAM, J., 1977. Discussion on "Cavity Expansions in Sands with curved envelopes" by Baligh. Proc. A.S.C.E., Vol.103, GT11, 1198-1200.

BUTTERFIELD, R. and ANDRAWES, K.Z., 1972. An investigation of a plane strain continuous penetration problem. Géotechnique, Vol.22, 597-617.

CHAPMAN, G.A. and DONALD, I.B., 1981. Interpretation of static penetration tests in sand. Proc. 10th I.C.S.M.F.E., Stockholm, Vol.2, 455-458.

DAVIDSON, J.L., MORTENSEN, R.A. and BARREIRO, D., 1981. Deformation in sand around a cone penetration tip. Proc. 10th I.C.S.M.F.E., Stockholm, Vol.2, 467-470.

DE RUITER, J., 1981. Current penetrometer practice, State-of-the-art report. Proc. A.S.C.E. National Convention, St. Louis, Missouri, Cone Penetration Testing and Experience, Edited by Norris, G.M. and Holtz, R.D., 1-48.

DURGUNOGLU, H.T., 1972. Static penetration resistance of soils. Ph.D. Thesis, University of California, Berkeley. (unpublished)

HOLDEN, J.C., 1971. Laboratory research on static penetrometers. University of Florida, Gainsville, Department of Civil Engineering, Internal Report CE-SM-71-1

HOLDEN, J.C., 1976. The determination of deformation and shear strength parameters for sands using the electrical friction cone penetrometer. N.G.I. Publication No.110, 55-60.

HOULSBY, G.T. and HITCHMAN, R., 1988. Calibration chamber tests of a cone penetrometer in sand. Géotechnique, Vol.38, No.1, 39-44.

JANBU, N. and SENNESET, K., 1974. Effective stress interpretation of in-situ static penetration tests. Proc. 1st E.S.O.P.T., Stockholm, Vol.2.2, 181-193.

JOUSTRA, K. and DE GIJT, J.G., 1982. Results and interpretation of cone penetration tests in soils of different mineralogical composition. Proc. 2nd E.S.O.P.T., Amsterdam, Vol.2, 615-626.

KERISEL, 1958. La mecanique des sols: recherches et investigations recentes. Rev. Trav. Paris, 874-878.

KOIZUMI, Y. et al (B.C.P. Committee), 1971. Field tests on piles in sand. Soils and Foundations, Vol.11, No.2, 29-49.

KOUMOTO, T. and KAKU, K., 1982. Three dimensional analysis of static cone penetration into clay. Proc. 2nd E.S.O.P.T., Amsterdam, Vol.2, 635-640

LEE, M.W., 1987. End bearing capacity of a pile in cohesionless soils. Ph.D. Thesis, University of Birmingham. (unpublished)

MEYERHOF, G.G., 1951. The ultimate bearing capacity of foundations. Géotechnique, Vol.2, 301-332

MEYERHOF, G.G., 1974. General report-Outside Europe. Proc. 1st E.S.O.P.T., Stockholm, Vol.2.1, 40-48.

MITCHELL, J.K. and LUNNE, T.A., 1978. Cone resistance as measure of sand strength. Proc. A.S.C.E., Vol.104, GT7, 995-1012.

MITCHELL, J.K. and KEAVENY, J.M., 1986. Determining sand strength by cone penetrometer. Proc. In-Situ '86, A.S.C.E. Specialty Conference. 823-839.

PARKIN, A.K., 1977. The friction cone penetrometer; Laboratory calibration for the prediction of sand properties. N.G.I. Internal Report 52108-5.

PARKIN, A.K. and LUNNE, T., 1982. Boundary effects in the laboratory calibration of a cone penetrometer for sand. N.G.I, Publication No.138, 307-312.

PEUCH, A., BIAREZ, J., CASSAN, M. and TOUTOUNGI, A., 1974. Contribution to the study of static and dynamic penetrometers. Proc. 1st E.S.O.P.T., Stockholm, Vol.1, 307-312.

PLANTEMA, G., 1957. Influence of density of sounding results in dry, moist and saturated sands. Proc. 4th I.C.S.M.F.E., London, Vol.1, 237-240

PRANDTL, L., 1920. Uber die Harte plastisher Korper. Nachrichten Kon. Gesell. der Wissenschaffen, Math. Phys. Klasse, Gottingen, 74-85.

ROBERTSON, P.K. and CAMPANELLA, R.C., 1983. Interpretation of cone penetration tests, Part I: sand, Part II: clay. Canadian Geotechnical Journal, Vol.20, No.4, 718-745.

ROBINSKY, E.I. and MORRISON, C.F., 1964. Sand displacement and compaction around model friction piles. Canadian Geotechnical Journal, Vol.1, No.2, 81-93.

SCHMERTMANN, J.H., 1972. Effect of in-situ lateral stress on friction cone penetrometer data in sand. Proc. Fugro Sondeer Symposium, published by Fugro-Cesco, Holland, 37-39.

SCHMERTMANN, J.H., 1975. Measurement of in-situ shear strength, state-of-the-art report. Proc. A.S.C.E. Conference on in-situ measurements of soil properties, Raleigh, NC. Vol.2, 57-138.

SMITS, F.P., 1982. Cone penetration tests in dry sand. Proc. 2nd E.S.O.P.T., Amsterdam, Vol.2, 877-881.

STEENFELT, J.S., RANDOLF, M.F. and WROTH, C.P., 1981. Instrumented model piles jacked into clay. Proc. 10th I.C.S.M.F.E., Stockholm, Vol.2, 857-864.

TCHENG, Y., 1961. Force portante des pieux. Proc. 5th I.C.S.M.F.E., Paris, Vol.3, 281.

TOMLINSON, M.J., 1987. Pile Design and Construction Practice (3rd ed.). A Viewpoint Publication, London, 378pp.

TREADWELL, D., 1975. Effect of layering on the cone resistance of soils. Ph.D. Thesis, University of California, Berkeley, CA (unpublished).

TROFIMENKOV, J.G., 1974. General report - Eastern Europe. Proc. 1st E.S.O.P.T., Stockholm, Vol.2.1, 24-28.

VEISMANIS, A., 1974. Laboratory investigation of electrical friction cone penetrometers in sand. Proc. 1st E.S.O.P.T., Stockholm, Vol.2.2, 407-419.

VESIĆ, A.S., 1963. Bearing capacity of deep foundations in sand. Highway Research Record 39, Highway Research Board, National Research Council, Washington D.C., 112-153.

VESIĆ, A.S., 1964. Investigation of bearing capacity of piles in sand. Proc. North American Conference on Deep Foundations, Mexico City.

VESIĆ, A.S., 1967. Ultimate loads and settlements of deep foundations in sand. Proc. Symposium on Bearing Capacity and Settlement of Foundation, Duke University, Durham, NC, 53-68.

VESIĆ, A.S., 1972. Expansion of cavities in infinite soil mass. Proc. A.S.C.E. Vol.98, SM3, 265-290.

VESIĆ, A.S., 1977. Design of pile foundations. National Cooperation Highway Research Program, Report No.42, Transportation Research Board, Washington, D.C.

VILLET, W.C.B. and MITCHELL, J.K., 1981. Cone resistance, relative density and friction angle. Proc. Cone Penetration Testing and Experience, Geotechnical Division, A.S.C.E., 178-207.

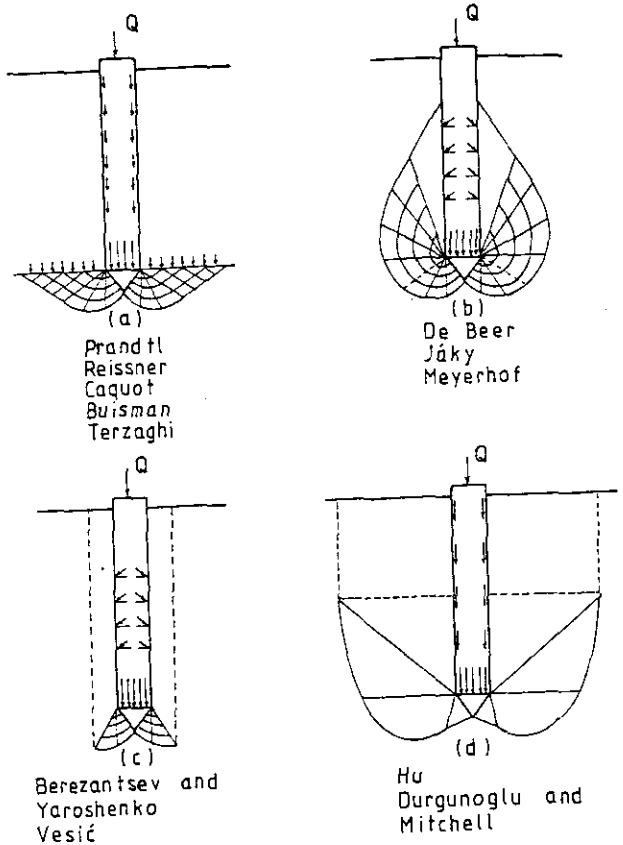

Fig.1 Mode of deformation assumed in different theoretical solutions (modified after Vesić, 1967)

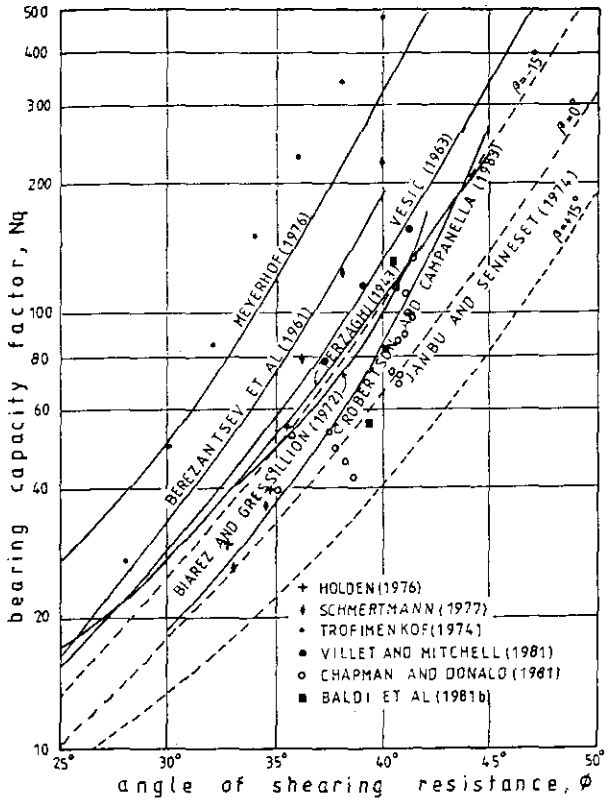

Fig.2 Variation of bearing capacity factor, Nq, suggested by different researchers

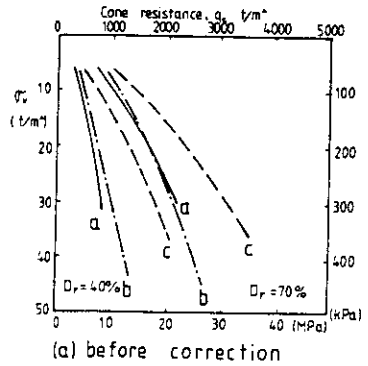

(a) before correction

a. Schmertmann (1976) Hilton Mines sand
b. Baldi et al (1982) Ticino sand
c. Villet and Mitchell (1981) Monterey sand

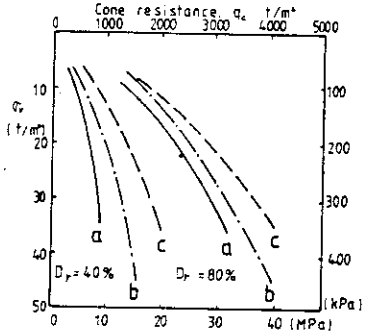

(b) after correction

uncorrected data after Baldi et al (1982)

corrected curves after Robertson and Campanella (1983)

Fig.3 Comparison of different relative density relationships

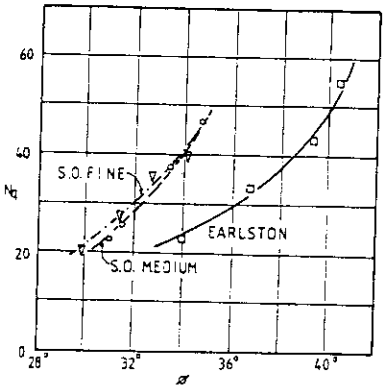

Fig.4 Angle of shearing resistance, Ø, vs. bearing capacity factor, Nq, for different sands (after Veismanis 1974)

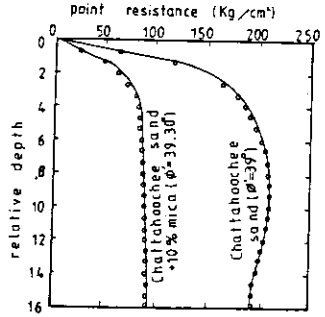

Note: Both tests were carried out at $\sigma_v = \sigma_h = 10.5$ t m (103 kPa)

Fig.5 Point resistance/sand and mica mixed sand (after Vesić, 1964)

Fig.7 Soil flow around piles and penetrometers (after AlAwkati, 1975)

Fig.6 Displacement and strains around a deep foundation in sand (after Robinsky and Morrison, 1964)

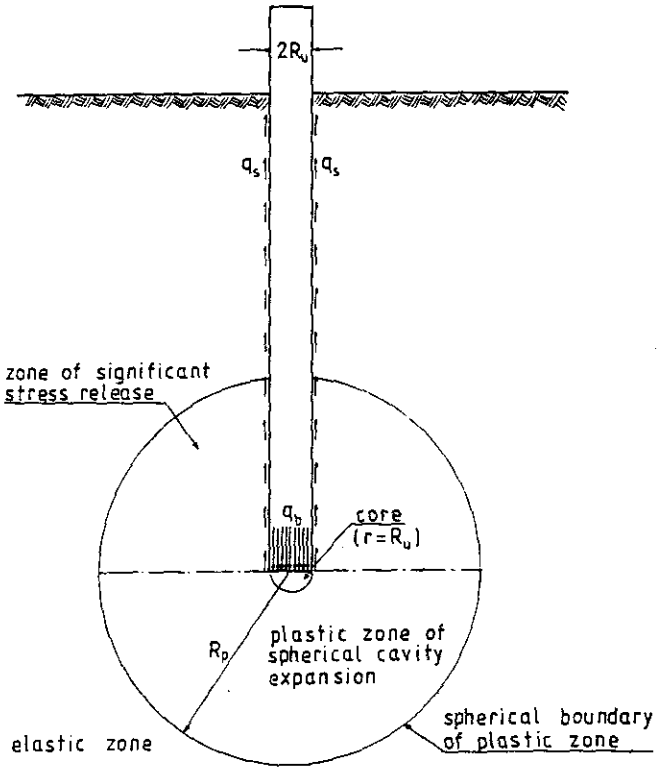

Fig.8 Assumed mode of deformation

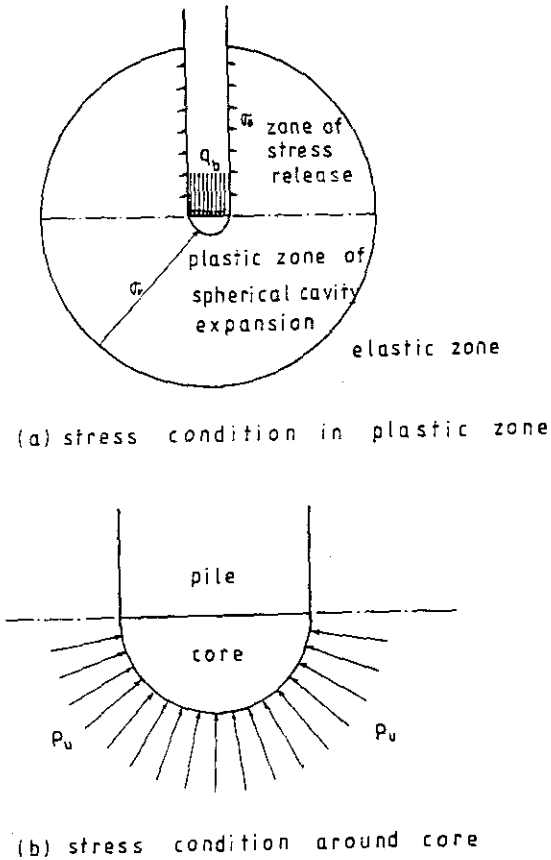

Fig.9 Stress conditions in plastic zone

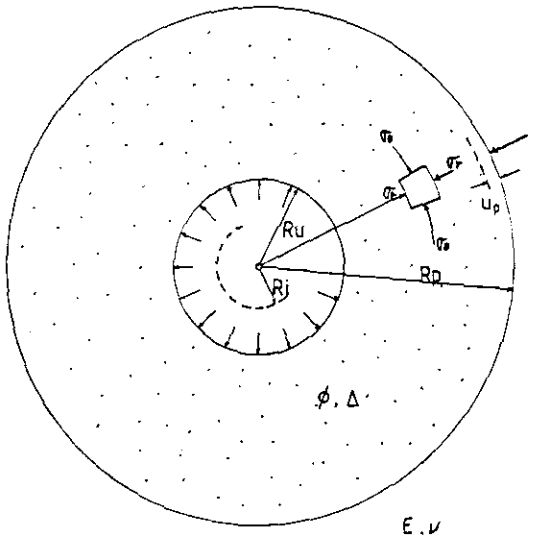

Fig.10 Expansion of spherical cavity (after Vesic, 1972)

Table 1 Summary of spherical cavity expansion solution

$$\frac{R_p}{R_u} = \sqrt[3]{\frac{I_r}{1+I_r.\Delta}}$$

$$I_r = \frac{E}{2(1+\nu).q.\tan\phi}$$

$$\frac{R_p}{R_u} = \sqrt[3]{I_{rr}}$$

$$I_{rr} = \frac{I_r}{1+I_r.\Delta}$$

$$P_u = \frac{3(1+\sin\phi)}{3-\sin\phi}\left(\frac{R_p}{R_u}\right)^{4\sin\phi/(1+\sin\phi)}.q$$

$$P_u = F_q.q$$

$$F_q = \frac{3(1+\sin\phi)}{3-\sin\phi}\,(I_{rr})^{4\sin\phi/3(1+\sin\phi)}$$

R_p = limit radial distance of plastic zone

R_u = limit radial distance of spherical cavity

I_r = rigidity index

I_{rr} = reduced rigidity index

P_u = limit spherical cavity expansion pressure

q = initial isotropic stress prior to pile driving

F_q = spherical cavity expansion factor

Δ = average volume change inside the plastic zone

E = Young's modulus

ν = Poisson's ratio

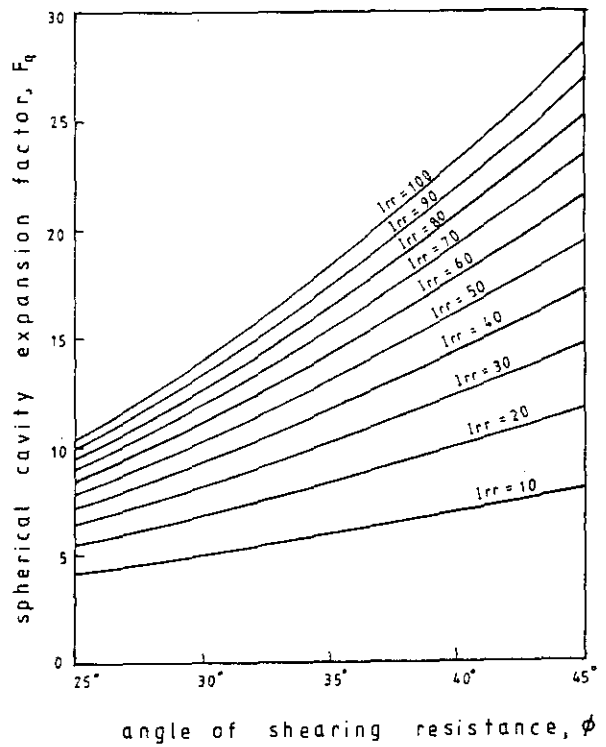

Fig.11 Spherical cavity expansion factor, F_q, for weak-grained soil (for straight failure envelope)

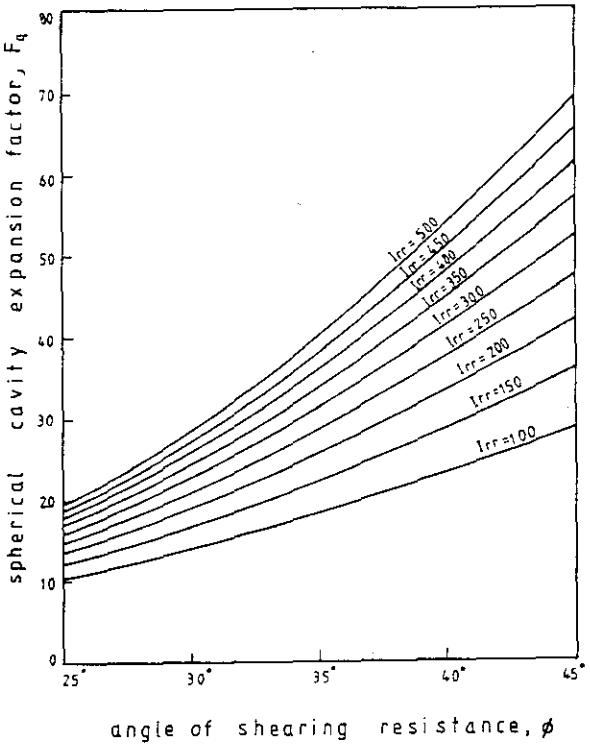

Fig.12 Spherical cavity expansion factor, F_q, for strong-grained soil (for straight failure envelope)

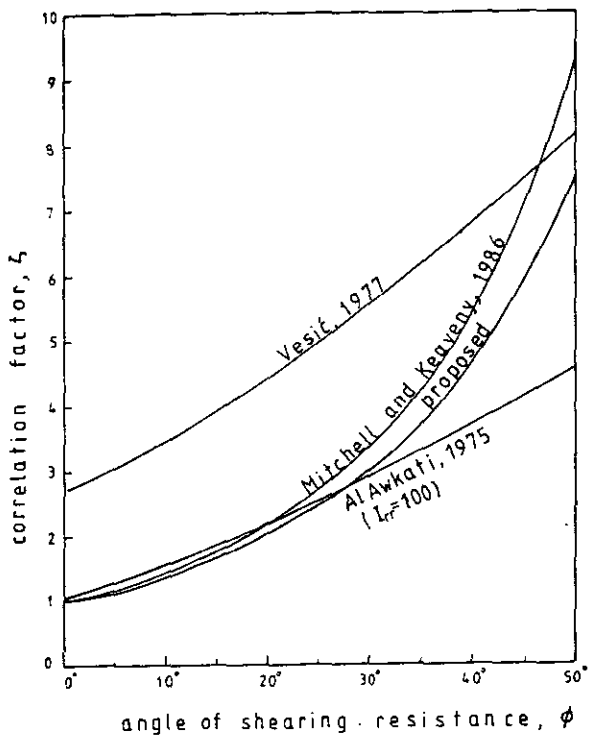

Fig.13 Correlation factor, ζ
(for straight failure envelope)

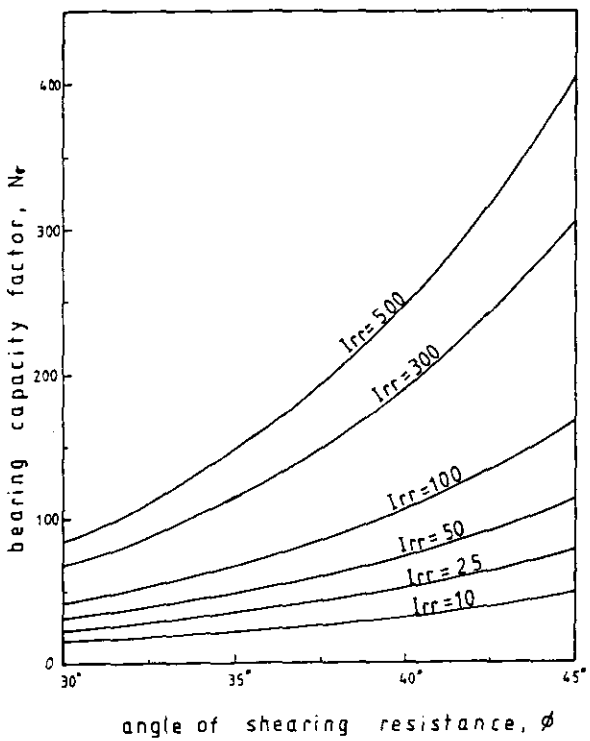

Fig.14 Bearing capacity factor, N_r
(for straight failure envelope)

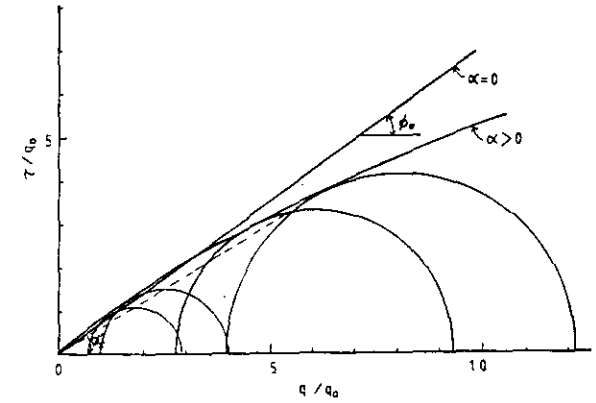

(a) Curved failure envelope

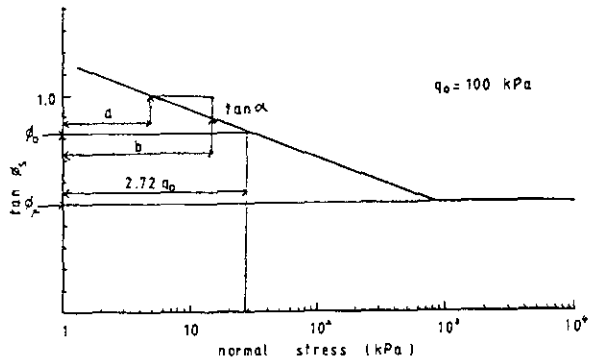

(b) Simplified tan ø vs. log q

Fig.15 Curvature of failure envelope (modified after Baligh, 1976)

Table 2 Calculation procedure

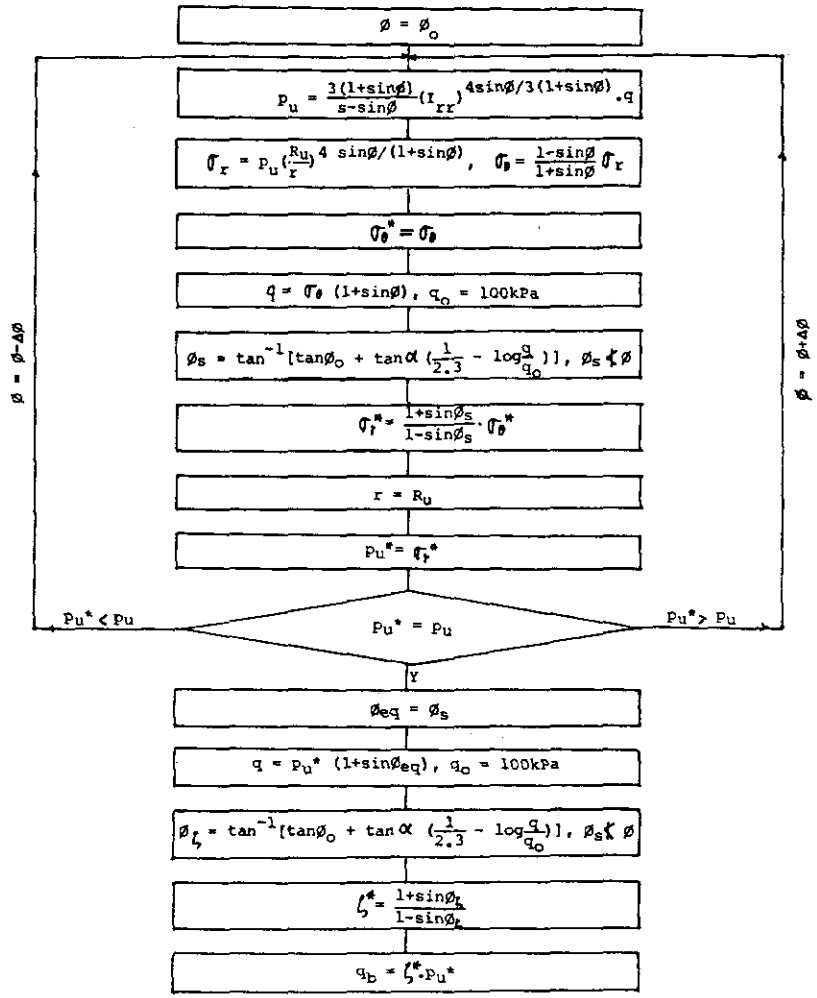

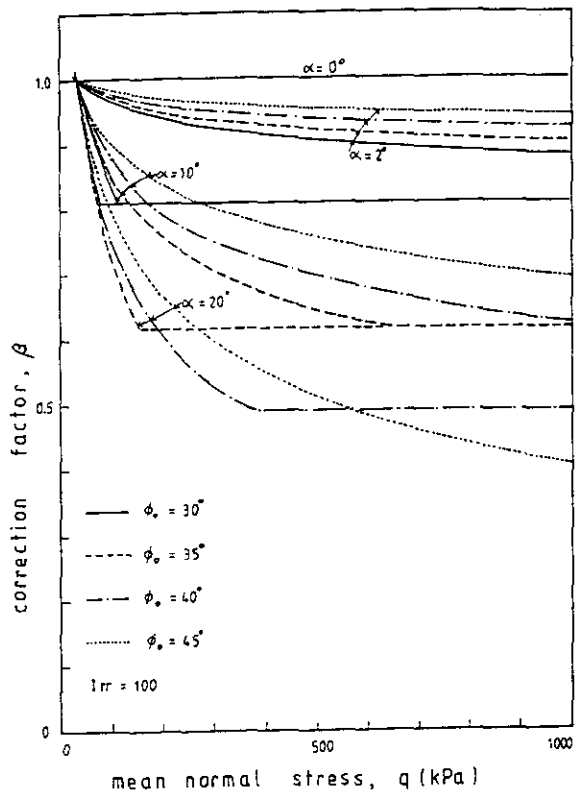

Fig.16 Variation of correction factor, β, with level of stress, q

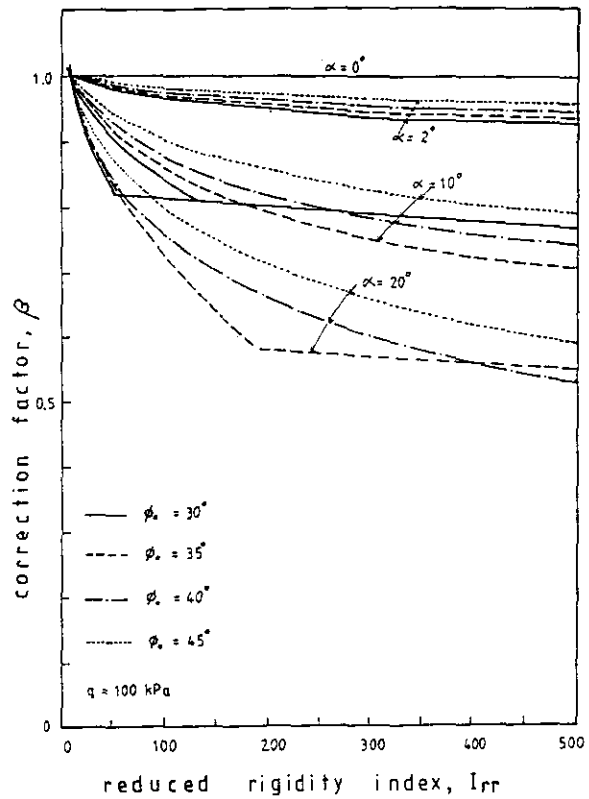

Fig.17 Variation of correction factor, β, with I_{rr}

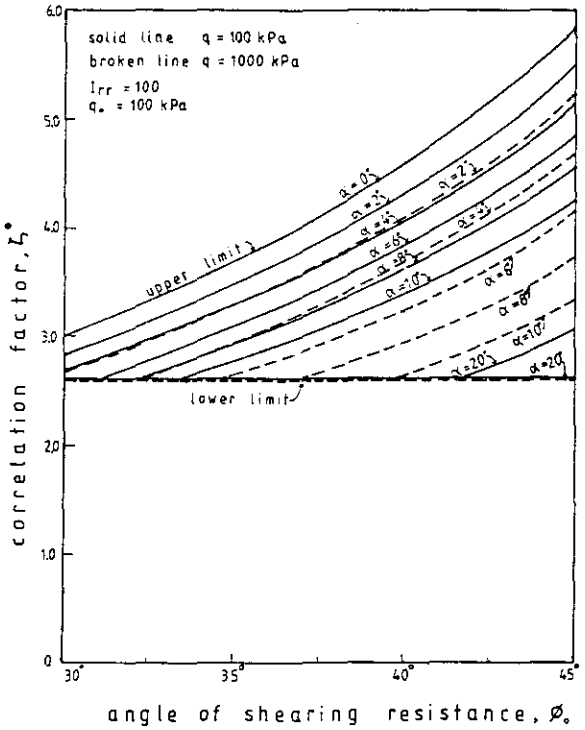

Fig.18 Variation of correlation factor, ζ^*

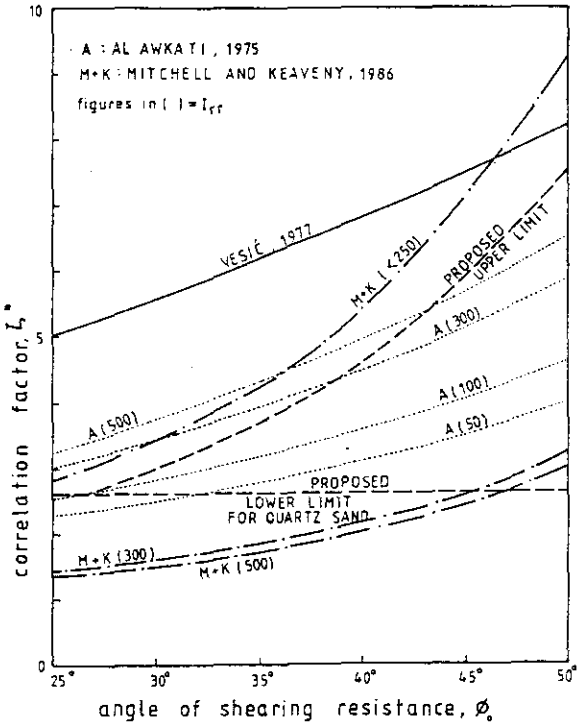

Fig.19 Comparison of correlation factor, ζ^*

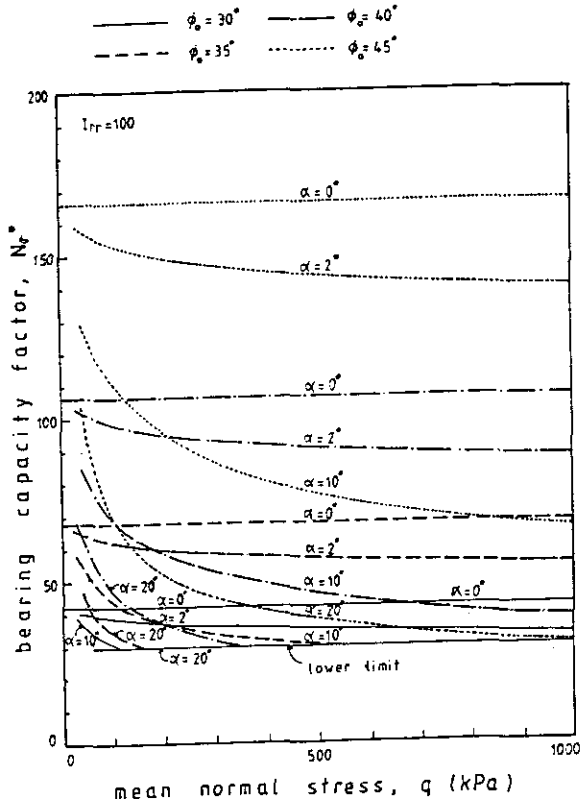

Fig.20 Variation of bearing capacity factor, $N_\sigma{}^*$, with q

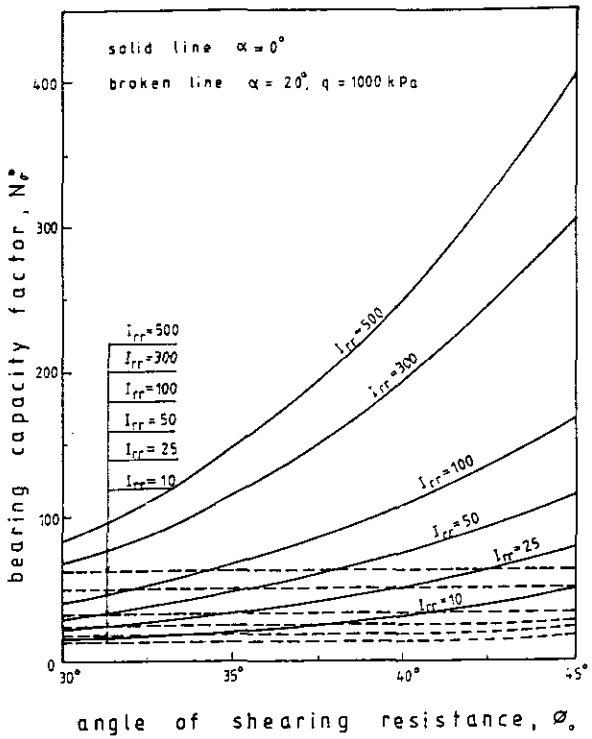

Fig.21 Variation of bearing capacity factor, N_σ^*

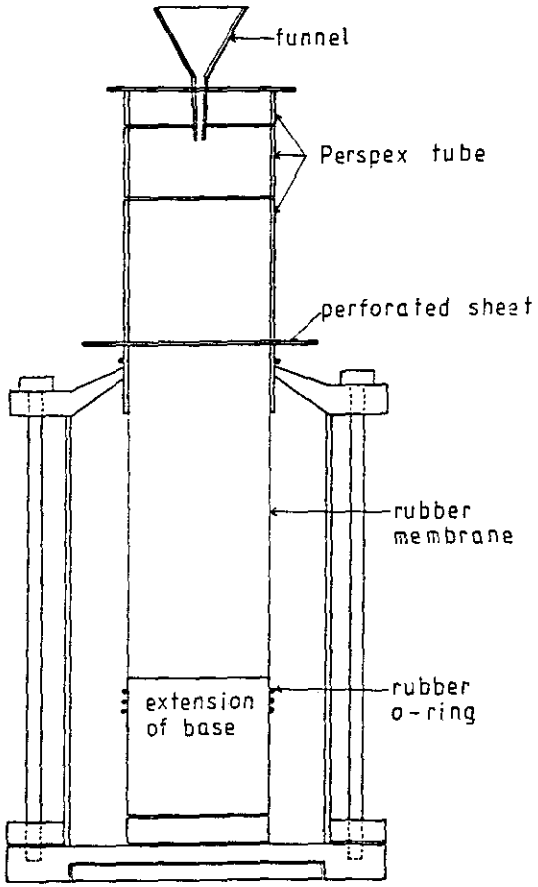

Fig.22 Sample preparation for mode for deformation study

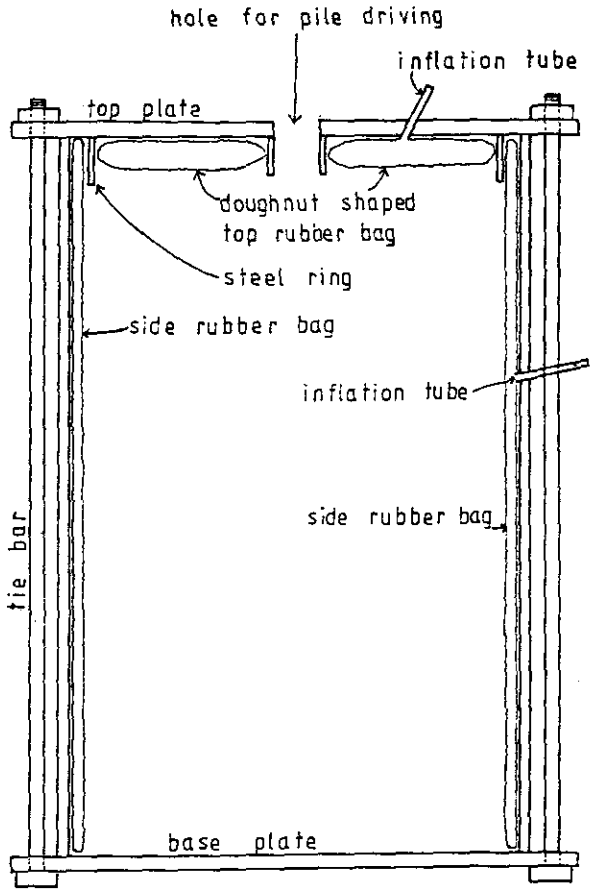

Fig.23 Calibration chamber detail

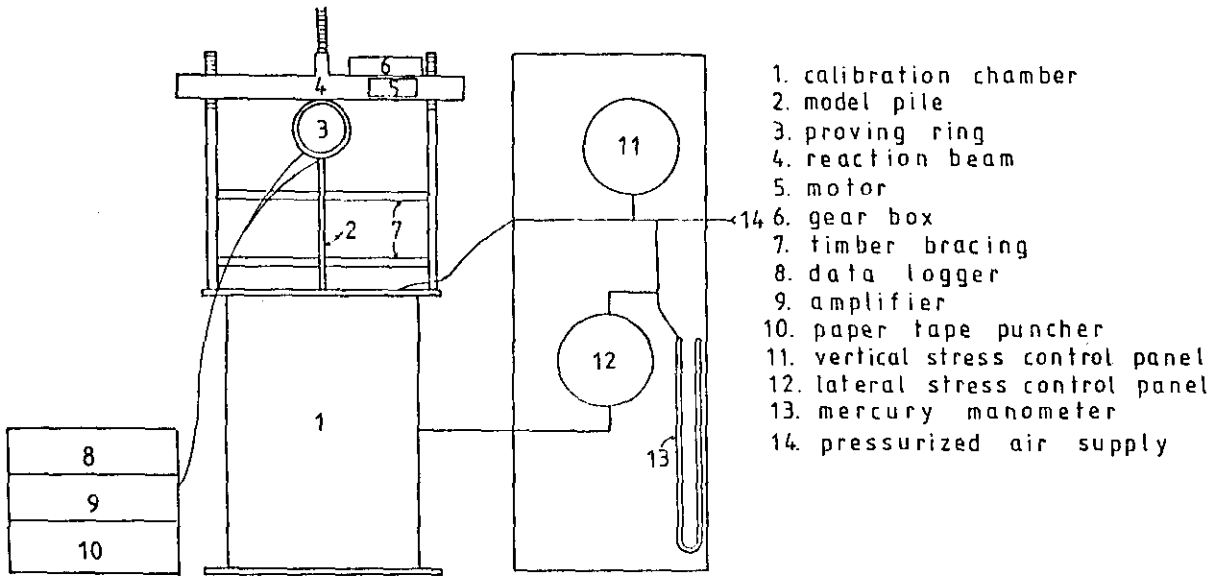

Fig.24 Experimental set up - model pile test

Table 3 Model pile penetration test results

Test No.	Specimen soil	σ_v kPa	σ_h kPa	q kPa	q_s MPa
1	quartz sand	50.00	20.75	30.50	1.87
2	quartz sand	100.00	41.50	61.00	
3	quartz sand	150.00	62.25	91.50	5.58
4	quartz sand	200.00	83.00	122.00	7.10
5	quartz sand	50.00	50.00	50.00	3.57
6	quartz sand	100.00	100.00	100.00	6.60
7	quartz sand	150.00	150.00	150.00	9.11
8	quartz sand	200.00	200.00	200.00	
9	anthracite (D_r=76%)	25.00	25.00	25.00	2.98
10	anthracite (D_r=76%)	50.00	50.00	50.00	3.97
11	anthracite (D_r=76%)	100.00	100.00	100.00	5.51
12	anthracite (D_r=76%)	150.00	150.00	150.00	6.47
13	anthracite (D_r=76%)	200.00	200.00	200.00	7.40
14	anthracite (D_r=64%)	50.00	50.00	50.00	3.39
15	anthracite (D_r=64%)	100.00	100.00	100.00	4.11
16	anthracite (D_r=64%)	150.00	150.00	150.00	5.36
17	anthracite (D_r=64%)	200.00	200.00	200.00	6.66
18	chalk	50.00	50.00	50.00	1.47
19	chalk	100.00	100.00	100.00	3.01
20	chalk	150.00	150.00	150.00	3.95

1 The result of test No.2 was discarded as the top bag had been folded during sample preparation.

2 The gear box had been broken during test No.8, and the result was discarded.

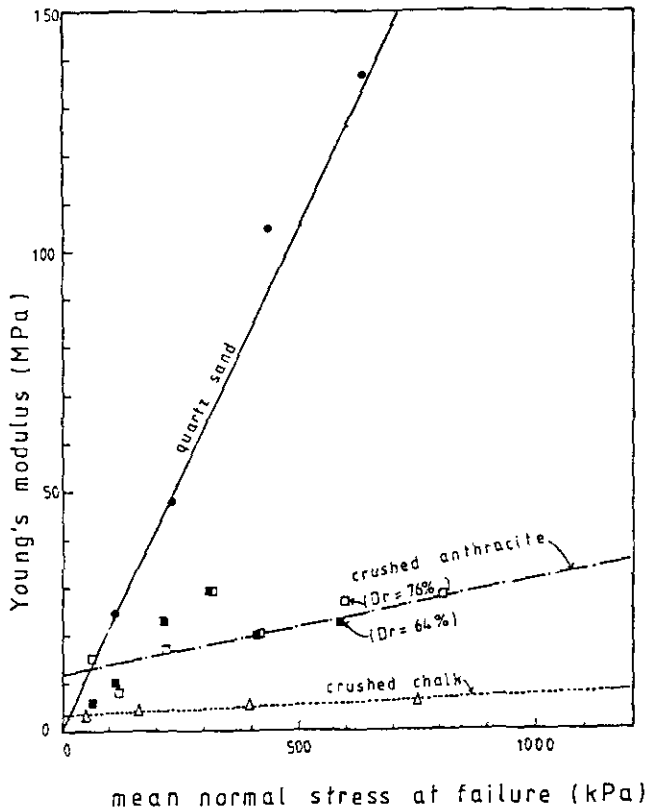

Fig.25 Determination of Young's modulus

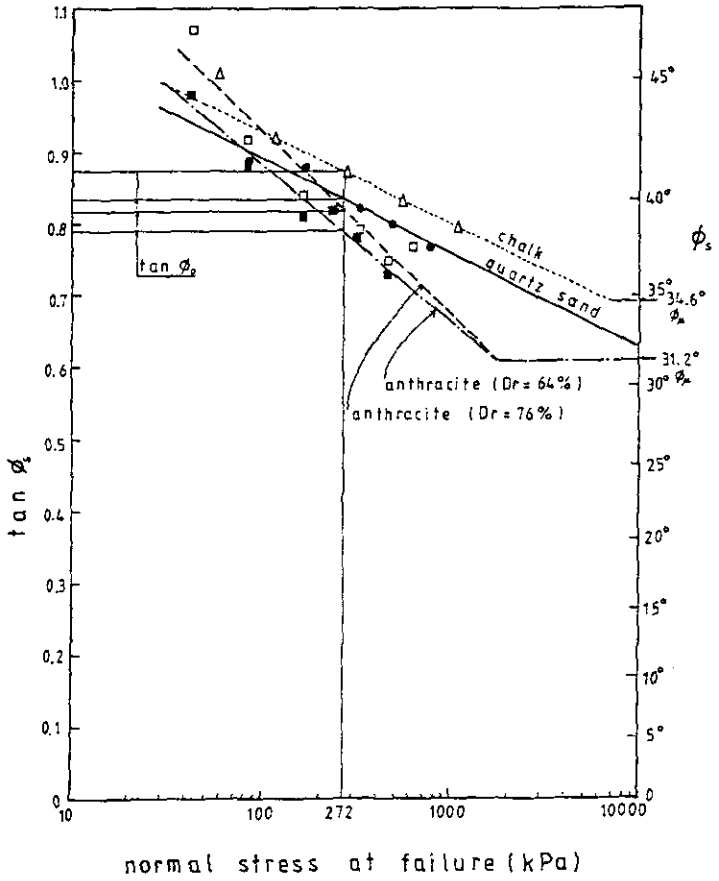

Fig.26 Determination of ϕ_o and α

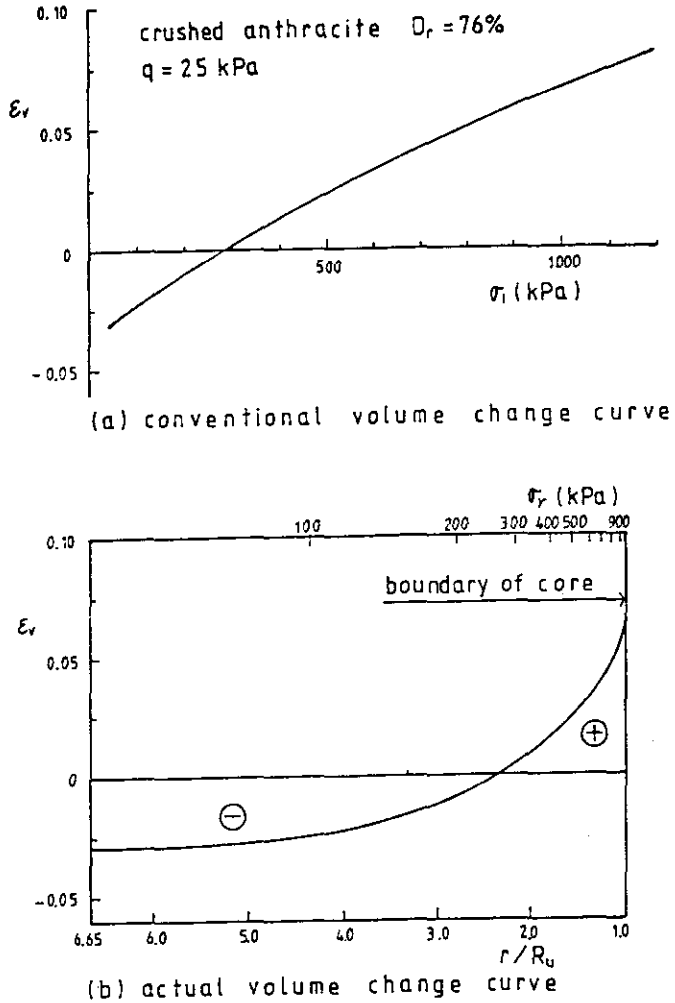

Fig.27 Actual volume change curve

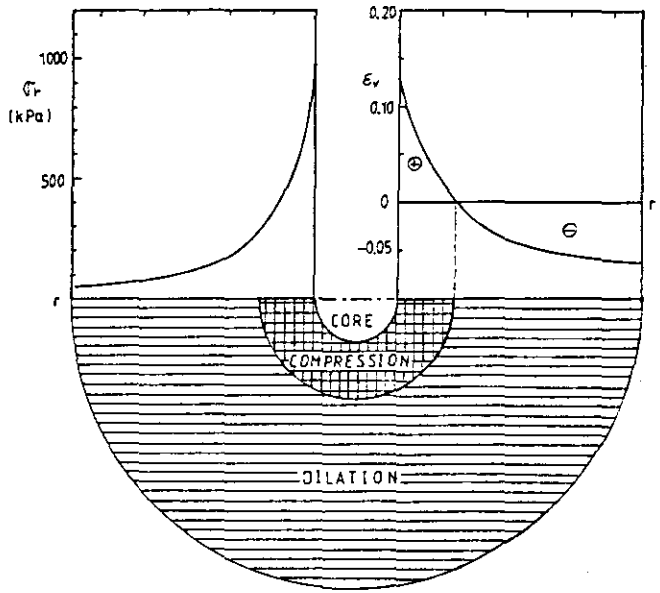

Fig.28 Estimation of average volume change for crushed anthracite D_r=76% q=25kPa

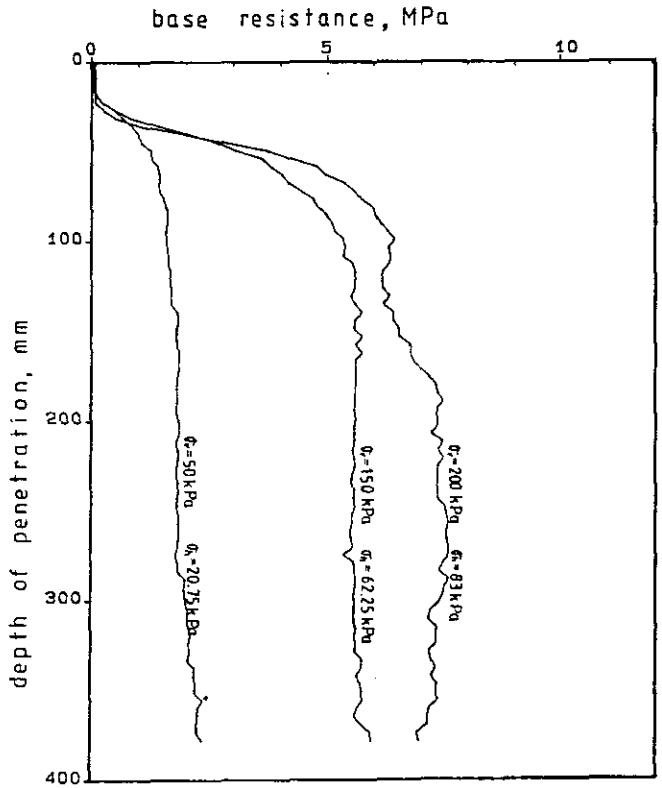

Fig.29 Penetration curves of quartz sand
K_o=0.415

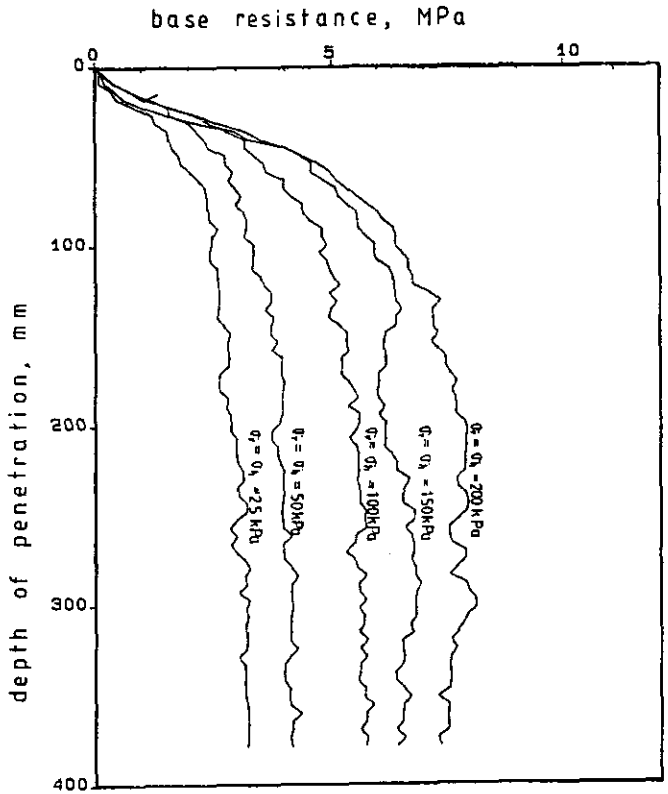

Fig.30 Penetration curves of crushed anthracite (D_r=76%)

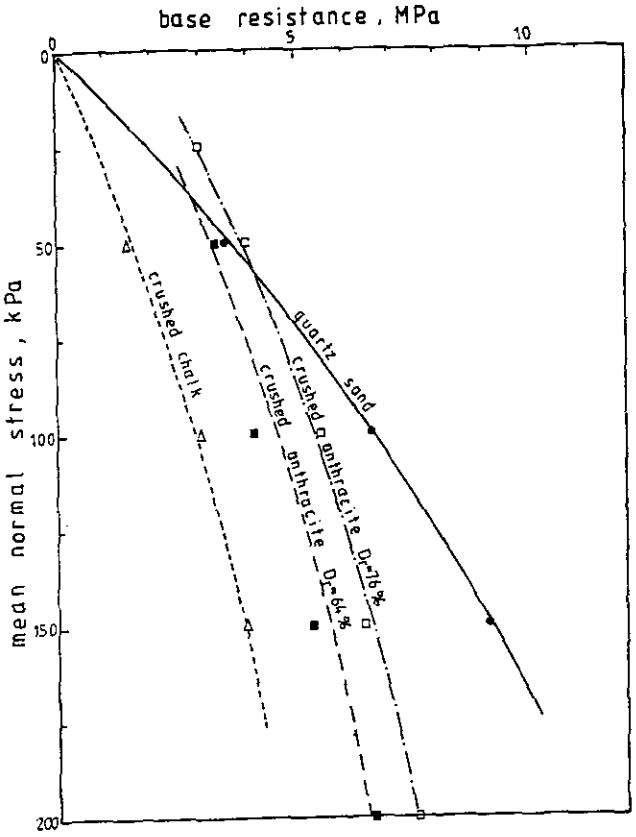

Fig.31 Measured base resistance

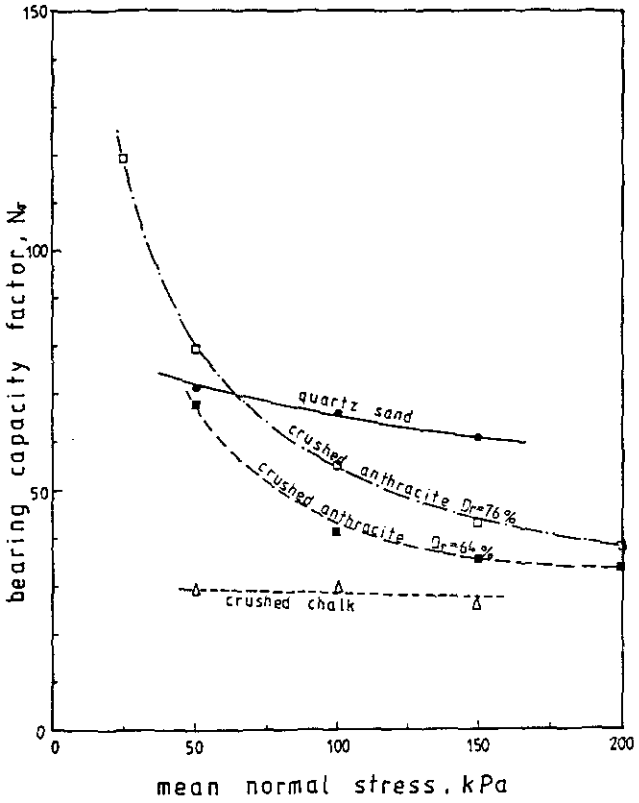

Fig.32 Measured bearing capacity factor

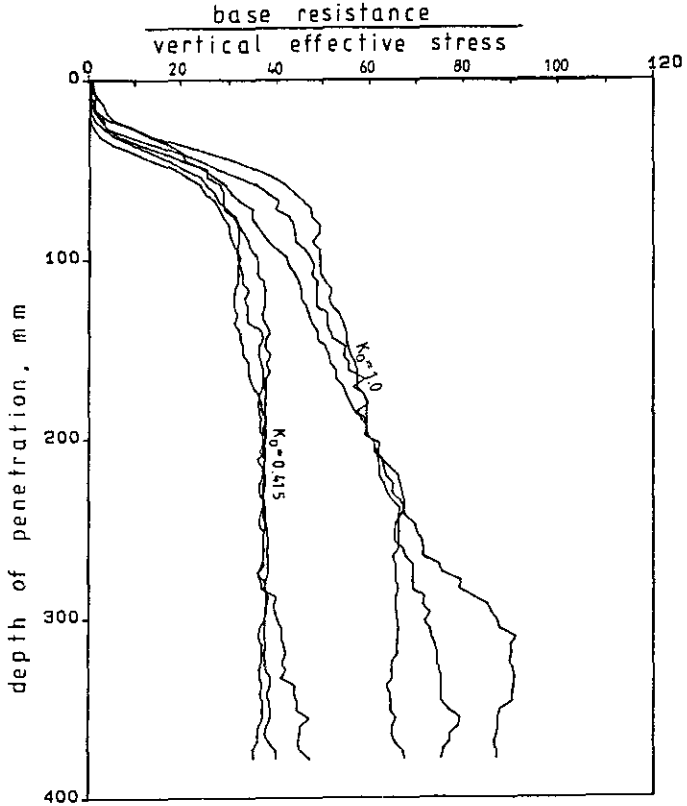

Fig. 33 base resistance / vertical effective stress

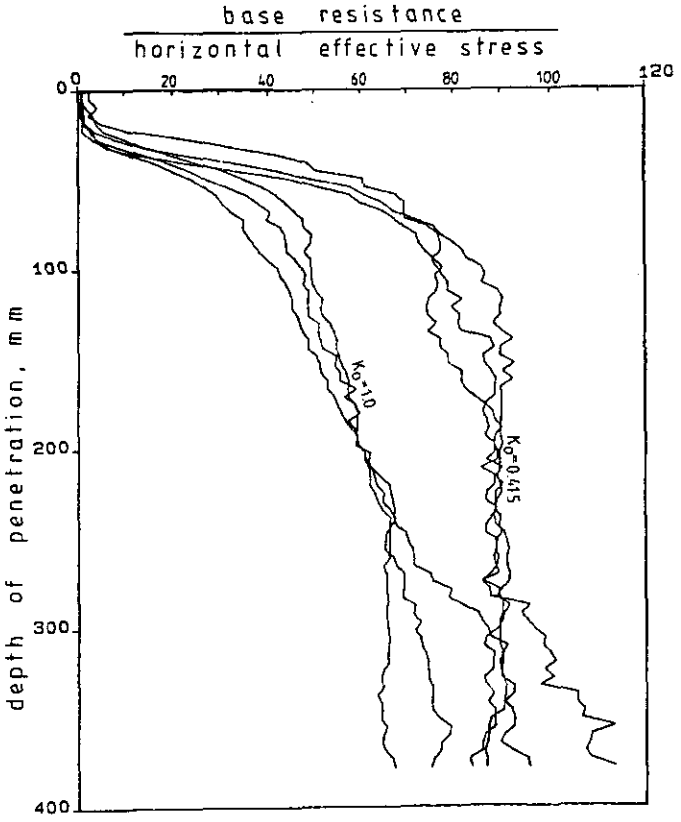

Fig.34 base resistance / Horizontal effective stress

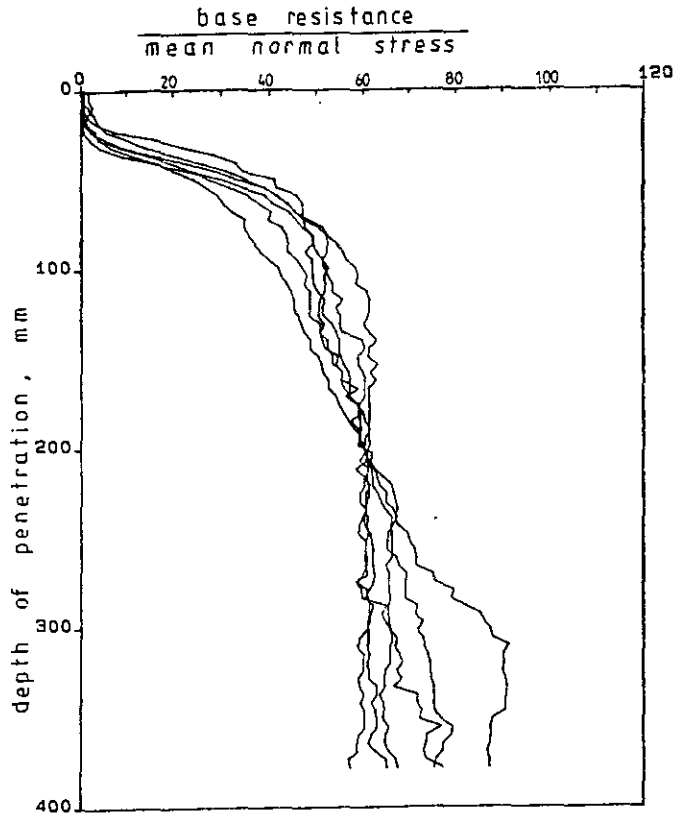

Fig.35 $\frac{\text{base resistance}}{\text{mean normal stress}}$

Table 4 Solutions considered in comparison

Solutions	Conditions	Sobmol
Vesić, 1977	s.f.e.	▽
Vesić, 1977	c.f.e.	▼
AlAwkati, 1975	s.f.e.	✱
Mitchell & Keaveny, 1986	s.f.e.	□
Mitchell & Keaveny, 1986	c.f.e.	■
Proposed	c.f.e.	●
Measured	-	○

* s.f.e.: straight failure envelope
c.f.e.: curved failure envelope

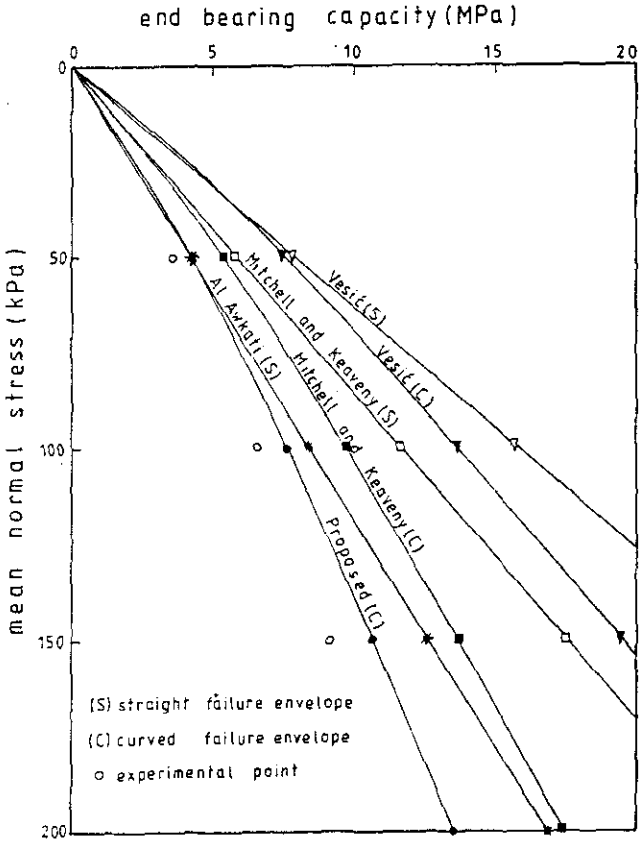

Fig.36 Comparison of predicted and measured end bearing capacity (quartz sand)

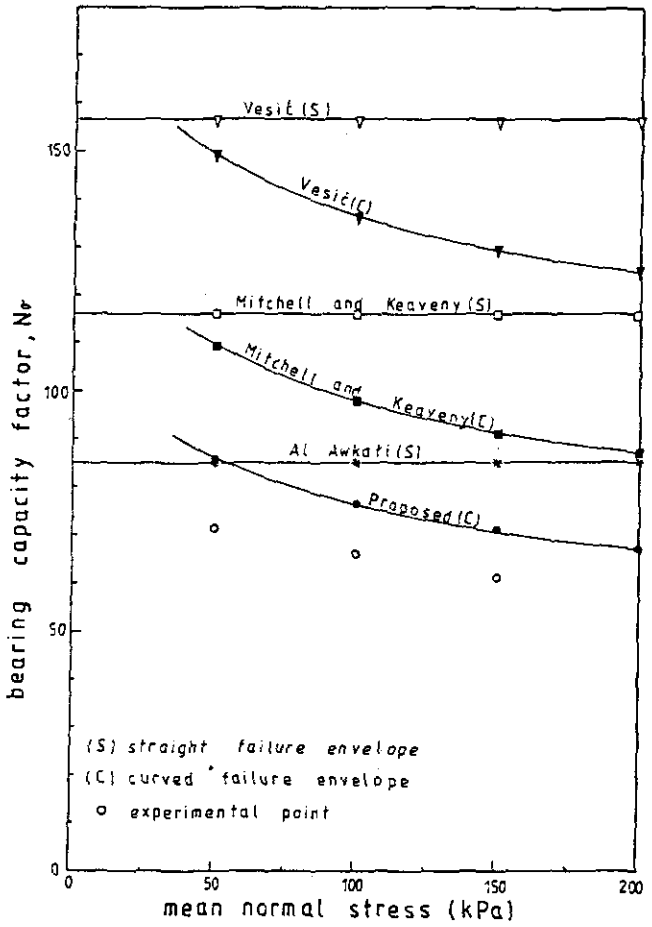

Fig.37 Comparison of bearing capacity factor (quartz sand)

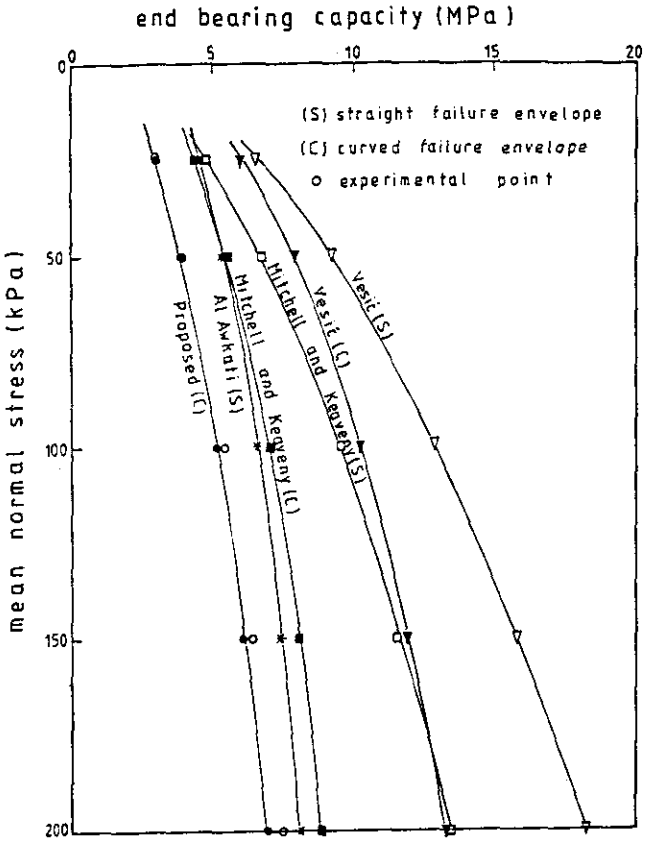

Fig.38 Comparison of predicted and measured end bearing capacity (crushed anthracite D_r=76%)

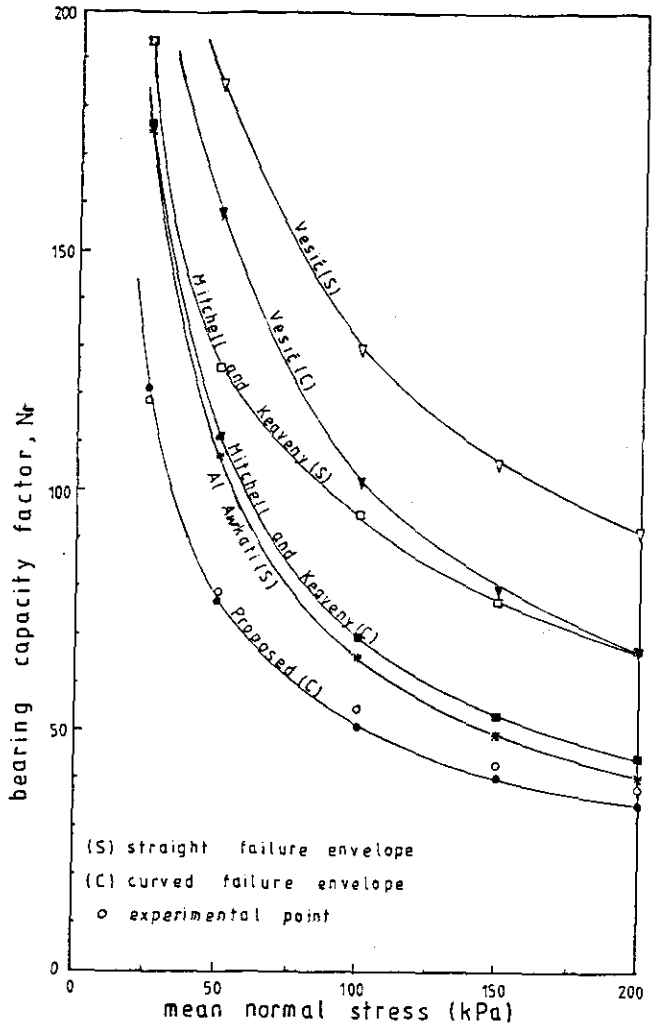

Fig.39 Comparison of bearing capacity factor (crushed anthracite D_r=76%)

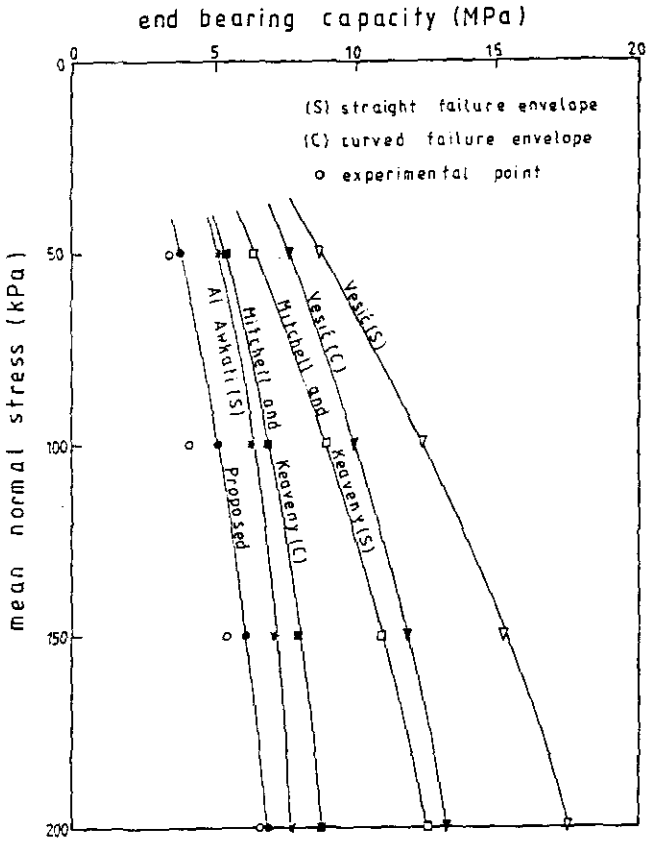

Fig.40 Comparison of predicted and measured end bearing capacity (crushed anthracite D_r=64%)

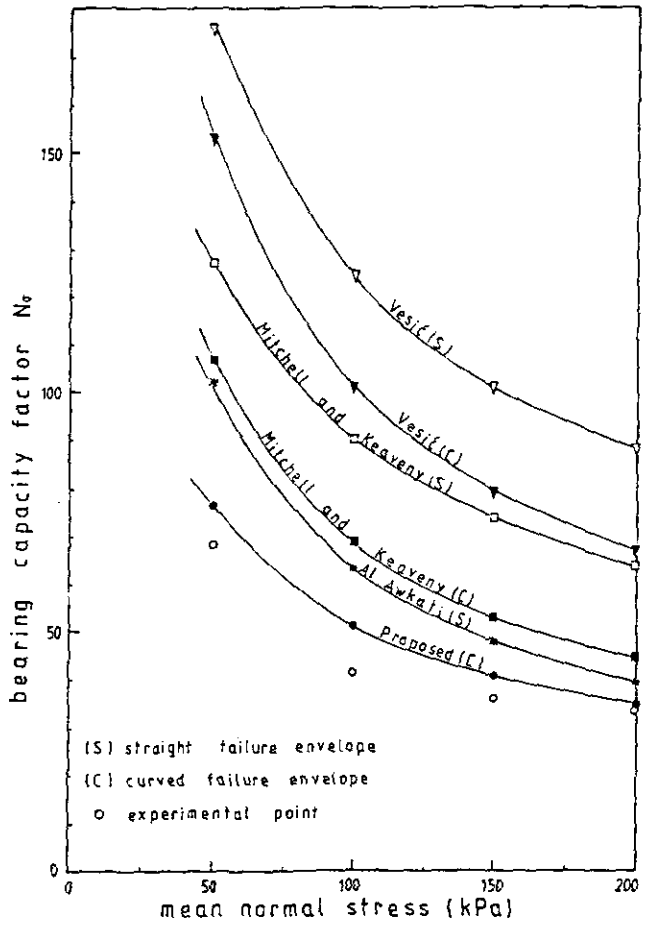

Fig.41 Comparison of bearing capacity factor (crushed anthracite D_r=64%)

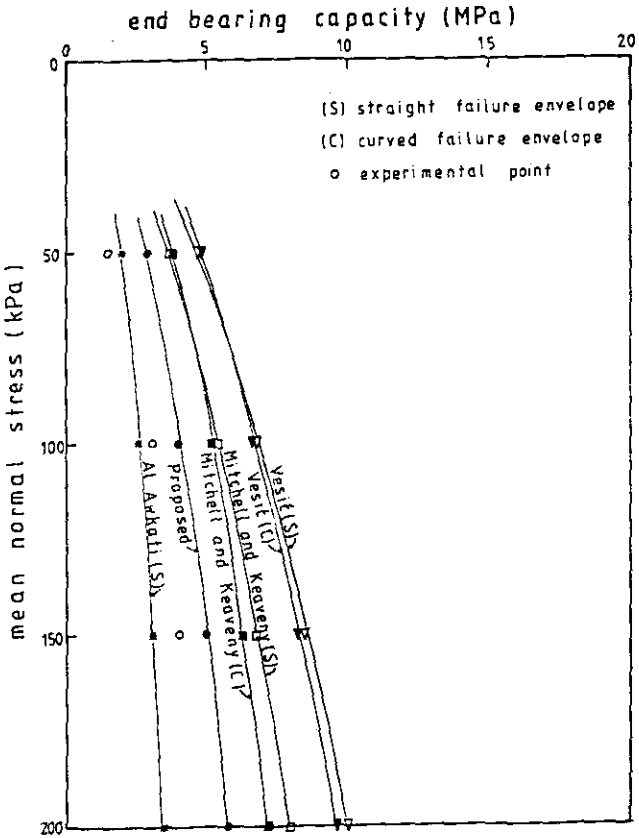

Fig.42 Comparison of predicted and measured end bearing capacity (crushed chalk)

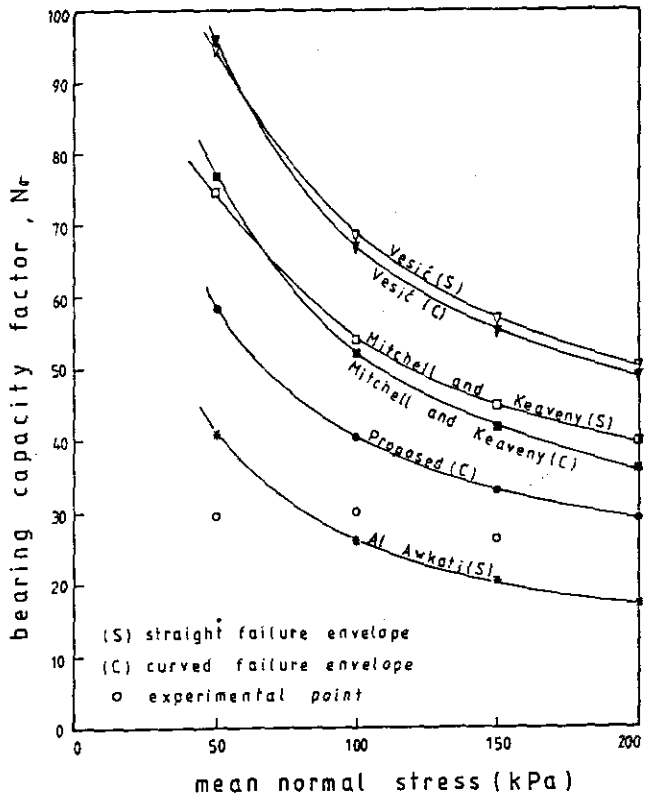

Fig.43 Comparison of bearing capacity factor (crushed chalk)

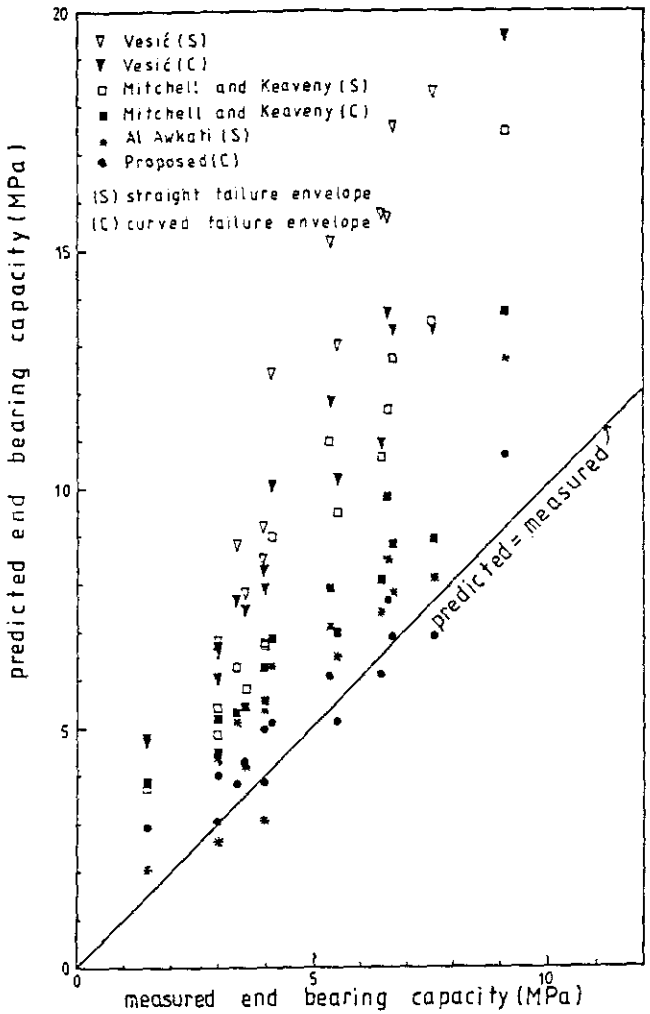

Fig.44 Comparison of predicted and measured end bearing capacity